QUANTIFICATION OF TRAFFIC-RELATED EMISSIONS AND EXPOSURES AT U.S.-MEXICO BORDER CROSSINGS USING REAL-TIME PORTABLE SENSORS

February 2024

CARTEEH

Center for Advancing Research in
Transportation Emissions, Energy, and Health
A USDOT University Transportation Center

Texas A&M Transportation Institute | Georgia Tech College of Engineering | Johns Hopkins Bloomberg School of Public Health | College of Engineering The University of Texas at El Paso | UC Riverside CE-CERT

Disclaimer

TECHNICAL REPORT DOCUMENTATION PAGE

1. Report No.	2. Government Accession No.	3. Recipient's Catalog No.
4. Title and Subtitle Quantification of traffic-related emissions and exposures at U.S.-Mexico border crossings using real-time portable sensors		5. Report Date February 2024 6. Performing Organization Code
7.Author(s) Mayra C. Chavez, Evan Williams, Leonardo Vazquez, Wen-Whai Li		8. Performing Organization Report No. 05-57-UTEP
9. Performing Organization Name and Address: CARTEEH UTC The University of Texas at El Paso 500 W. University Ave, El Paso, TX 79968		10. Work Unit No. 11. Contract or Grant No. 69A3551747128
12. Sponsoring Agency Name and Address Office of the Secretary of Transportation (OST) U.S. Department of Transportation (USDOT)		13. Type of Report and Period Final 03/01/2021-03/31/2023 14. Sponsoring Agency Code

15. Supplementary Notes
This project was funded by the Center for Advancing Research in Transportation Emissions, Energy, and Health University Transportation Center, a grant from the U.S. Department of Transportation – Office of the Assistant Secretary for Research and Technology, University Transportation Centers Program.

16. Abstract

Air monitoring was conducted at the Bridge of the Americas (BOTA) in El Paso, Texas, using continuous Federal Equivalent Method (FEM) instruments for four criteria pollutants ($PM_{2.5}$, PM_{10}, O_3, and NO_2) to assess exposure levels of facility operators and users of the BOTA. Concurrent monitoring of $PM_{2.5}$ in the nearby community using low-cost sensors provided citizens with real-time pollution levels. Air dispersion modeling was conducted using seasonal traffic emission rates to predict $PM_{2.5}$, PM_{10}, and NO_2 levels at the BOTA and the surrounding areas. Monitored average concentrations at the BOTA of $PM_{2.5}$, O_3, and NO_2 were 2 percent higher, 15 percent lower, and 20 percent higher, respectively, than concentrations observed at a nearby reference station 0.4 km away. The dispersion modeling of wait-time effects at the BOTA showed that on-site air pollution reaches a maximum level when the queue length is 270 m and concentrations decrease tenfold as the cross-BOTA distance reaches 200 m. Modeled estimates indicate that individuals traveling along the pedestrian walkway experience 75 percent of the impact of the emissions relative to the concentrations inside the BOTA. Modeled estimates indicate that toll booth workers experience 66 percent of the pollutant concentrations estimated inside the traffic lanes of the BOTA. The modeled emissions contribute 51, 147, and 7 percent of the monitored all-period averaged $PM_{2.5}$, PM_{10}, and NO_2 concentrations, respectively. Modeled concentration estimates provide a spatial heat map to assess the reach and direction of pollution exposure.

17. Key Words	18. Distribution Statement
Air pollution, Transportation data, Traffic volume, Air dispersion modeling	No restrictions. This document is available to the public through the CARTEEH UTC website. http://carteeh.org

19. Security Classif. (of this report)	20. Security Classif. (of this page)	21. No. of Pages	22. Price
Unclassified	Unclassified	57	$0.00

Form DOT F 1700.7 (8-72) Reproduction of completed page authorized

Executive Summary

1. Problem statement:

Traffic congestion and long wait times at border crossings and ports of entry (POEs) have especially increased during the COVID-19 pandemic due to staff shortages and lane closures on the bridges. Evaluating the effects of border crossing related emissions on the region can provide further information to address the improvement in air quality through targeted urban policy interventions. As the urban area looks to expand, it is important that cities integrate public health perspectives into the planning phase of transportation infrastructure development.

This study is concerned with the potential air pollution impacts on the health of bridge users (i.e., pedestrian, commuters, commercial truck drivers) and POE workers (i.e., U.S. Customs and Border Protection agents, federal law enforcement workers). This project will address the transportation-related emissions and health concerns of those citizens and workers present at these POEs by collecting and analyzing exposure data for bridge workers, pedestrians, vendors, and at the check point. Emission impacts to the nearby communities will be addressed by analyzing the data collected using a network of low-cost air sensors.

2. Technical objectives:

- Establish the baseline exposure concentrations for POE workers and users.
- Evaluate the pollution impacts of POE emissions on the nearby community using concurrent monitoring and by collecting and analyzing pollutant data at the traffic lanes on the BOTA.

3. Key findings:

We have quantified the exposure concentrations of $PM_{2.5}$, O_3, and NO_2 for the BOTA workers and users. The air dispersion modeling of the POE wait time on pollution levels at the BOTA showed that modeled on-site air pollution stabilizes to a maximum at a queue length of approximately 270 m. The BOTA operators deployed at the POE are expected to be exposed to the maximum levels of pollution when the queue length exceeds 270 m from the toll booth locations. In addition, modeled air pollution disperses rapidly as the lateral distance from the center of the BOTA increases. The modeled air pollutant concentrations decrease by approximately tenfold as the cross-BOTA distance increases to 200 m, indicating that pedestrians and near-road BOTA workers should maintain distances up to this level to experience less impact from the BOTA traffic-related emissions. Modeled estimates indicate that individuals traveling along the pedestrian walkway may experience 75 percent of the impact of the BOTA emissions relative to the concentrations inside the BOTA. The modeled BOTA emissions were found to contribute 51 percent, 147 percent, and 7 percent of the monitored all-period averaged $PM_{2.5}$, PM_{10}, and NO_2 concentrations, respectively.

4. Project impacts:

Our results suggest that traffic emissions do not result in elevated levels of pollutant concentrations at this POE compared to the concentration levels observed in the nearby community. In addition, the performance and accuracy of the low-cost sensors appear to be less reliable during our study, although the devices were capable of detecting the trends and variability in pollutant concentrations in real time. We have shown that in-traffic air pollution at a busy international POEs does not exceed its respective NAAQS and therefore may pose insignificant health risks to the transportation facility users and workers. Further studies at more POEs will help validate our findings.

This study also addresses the spatial and temporal concentration variations in a community near a POE resulting from traffic and idling emissions on a microscale. However, modeled impacts of the traffic emissions on the air quality subside rapidly with increasing distance away from the highway.

Acknowledgments

This project was supported by a grant from the U.S. Department of Transportation (USDOT) through the Center for Advancing Research in Transportation Emissions, Energy, and Health (CARTEEH). We thank the U.S. Customs and Border Protection (U.S. CBP) for their assistance. We also thank Mr. Sergio Vasquez and Eddie Moderow of the Texas Commission on Environmental Quality (TCEQ) and Mr. Alan Wiernicki, Mr. Ernesto Ortiz, Mr. Abel Carreon, and Mr. Joe Parga of El Paso Independent School District (EPISD) for their assistance in setting up the low-cost sensors on EPISD campuses.

The contents of this paper are solely the responsibility of the authors and do not necessarily represent the official views of the USDOT, TCEQ, or U.S. CBP.

Table of Contents

List of Figures ..... **vii**

List of Tables ..... **viii**

Background and Introduction **1**

Methodology **3**

Study Design and Site Selection 3

Instrumentation and Correction 4

Data Collection 5

AERMOD Dispersion Modeling of BOTA Emission 6

AERMOD Modeling Setup 8

Modeling Setup 8

Modeling Scenarios 11

Analysis of BOTA Air Pollution Data 17

$PM_{2.5}$ Concentrations in the Community 22

Comparison of BOTA and TCEQ Measurements 27

TRAP Concentration on the BOTA 30

Comparison of BOTA and Near-Road Community Measurements 30

Data Correction 30

$PM_{2.5}$ in the Community 32

Concentration Estimates Predicted by AERMOD Modeling 33

Impacts of Queue Length on Exposure Concentrations 33

Cross-Roadway Concentration Distribution 34

Comparison of Modeled and Monitored Concentrations Using Calculated Seasonal Emission Rates 35

Assessment of Community Exposure Resulting from the BOTA Emissions 37

Summary and Future Research **45**

References **47**

List of Figures

Figure 1. BOTA air pollution collection stations (a) overhead view, (b) Station A, and (c) Station B. 3

Figure 2. Map of air pollution collection sites. 4

Figure 3. Wind roses at CAMS sites. 6

Figure 4. Similarity of wind patterns at CAMS 41 and BOTA; (a) locations of CAMS 41 and BOTA Met and (b) wind rose plots at CAMS 41 and BOTA Met (Olvera et al., 2011). 6

Figure 5. AERMOD model data flow. 7

Figure 6. Volume source set-up. 10

Figure 7. AERMOD area source and receptor model set-up. 11

Figure 8. Queue length analysis. 14

Figure 9. Average wait times for February and March at the BOTA. 15

Figure 10. Pearson correlations between Stations A and B at the BOTA. 17

Figure 11. Weekday hourly variation of (a) $PM_{2.5}$, (b) O_3, (c) Station A NO_2, and (d) Station B NO_2 at the BOTA, where the distribution of data for the hour are marked in terms minimum (Q1-1.5•IQR), first quartile (Q1), median, third quartile (Q3), and maximum (Q3 + 1.5 IQR). 20

Figure 12. Weekend hourly variation of (a) $PM_{2.5}$, (b) O_3, (c) Station A NO_2, and (d) Station B NO_2 at the BOTA. 21

Figure 13. Community Purple Air $PM_{2.5}$ time series data and concurrent wind data. (Data collected from collocated monitors are colored in orange.) 26

Figure 14. Pearson correlations between BOTA and CAMS 41 data: (a) $PM_{2.5}$, (b) O_3, (c) Station A NO_2, and (d) Station B NO_2. 27

Figure 15. Time series of (a) $PM_{2.5}$, (b) O_3, and (c) NO_2 concentrations at BOTA and CAMS 41. 29

Figure 16. $PM_{2.5}$ concentration roses at BOTA and CAMS 41 sites. 30

Figure 17. MLR corrected data and SLR corrected data compared to reference data. 32

Figure 18. $PM_{2.5}$ box plots for community Purple Air $PM_{2.5}$ data. 33

Figure 19. Queue analysis of modeled results at monitoring sites. 34

Figure 20. Cross-roadway receptor placement 34

Figure 21. Modeled $PM_{2.5}$ dispersion as a function of distance from the highway. 35

Figure 22. Hourly modeled and monitored results: (a) $PM_{2.5}$, (b) PM_{10}, and (c) NO_2. 36

Figure 23. 24-hr averages of modeled and monitored data. 37

Figure 24. Period average, max 1-hr, and max 24-hr PM2.5 concentration estimates. 40

Figure 25. Period average, max 1-hr, and max 24-hr Pm_{10} concentration estimates. 41

Figure 26. Period average, max 1-hr, and max 24-hr No_2 concentration estimates 41

List of Tables

Table 1. Summary of Purple Air Locations. 4

Table 2. Correction Statistics against FRM Instruments for the Instruments Used at the BOTA. 5

Table 3. Steps in Modeling Approach. 8

Table 4. Queue Length Analysis Scenario Descriptions. 13

Table 5. Running Emissions Rates for Winter Season at 2.5 mph. 15

Table 6. Emissions Rates by Source Area Size, Weekday/Weekend, and Pollutant. 16

Table 7. Descriptive Statistics for TRAP Concentrations Measured at the BOTA. 19

Table 8. Period Summary Statistics for Regional Monitoring Stations in Comparison with BOTA Data. 28

Table 9. Period Summary Statistics 28

Table 10. Daylight Hours (6 a.m.–6 p.m.). 28

Table 11. Night Hours (7 p.m.–5 a.m.). 28

Table 12. Purple Air Correction Regression Analysis. 32

Table 13. Descriptive Statistics of Modeled and Monitored Data (Period Average). 39

Table 14. Descriptive Statistics of Modeled and Monitored Data (1-hr Max). 39

Table 15. Descriptive Statistics of Modeled and Monitored data (24-hr Max). 40

Background and Introduction

Vehicular emissions of transportation-related air pollutants (TRAPs) at international ports of entry (POEs) have been a major health concern for the users of the facilities as well as residents of nearby communities. Excessive emissions at low or idle speeds from vehicles crossing the border are exacerbated by the long wait times for immigration and security inspection at the POEs. The problem is common not only to the U.S.-Mexico border region but also in the northern U.S.-Canada border region. Studies have shown that residents of communities in close proximity to the U.S.-Canada trade corridors are potentially exposed to increased commercial traffic pollution (Baxter et al., 2008). For instance, Detroit, Michigan, and Windsor, Ontario, a border area separated by the Detroit River and connected by the Detroit-Windsor Tunnel and the Ambassador Bridge, one of the busiest commercial international border crossings in North America, is classified as a high pollution zone due to industrial and transportation emissions (Miller et al., 2010). In the U.S.-Mexico region, 13 sister cities experience air pollution problems resulting from cross-border traffic. The San Ysidro POE between San Diego, California, and Tijuana, Baja California, Mexico, which is the busiest land-based international border crossing in the world, is considered a major source of exposure risk to the San Ysidro community (Quintana et al., 2014). In El Paso, Texas, there are four international POEs between the United States and Mexico. According to the U.S. Department of Transportation, 15 to 16 million passenger cars and 750,000 commercial vehicles cross the four POEs between El Paso, Texas, and Cd. Juárez, Chihuahua each year. The vehicle fleet at these POEs is a complicated mixture of local passenger vehicles and commercial trucks. The international POEs are significant sources of emissions for hazardous air pollutants and could pose a serious health threat to nearby residents, custom inspectors, and bridge users. Quintana et al. (2018) collected air quality data on particulate matter from monitoring sites near the border and concluded that identifying border crossing as a significant source of air pollution could not be done due to the distance of the monitors in relation to the border. The study outlined the need to include air quality monitoring at or close to the sources at the POEs. Unfortunately, few air quality studies have been conducted at the POEs due to concerns of security compromise, traffic interruption, and vandalism.

The pollution problem at the POEs has become more pronounced in recent years due to the increased volume of traffic and prolonged wait time for the U.S. custom border inspection, resulting in large numbers of vehicles idling in queues that may last hours. Drivers sitting in vehicles waiting to cross the POEs and custom agents or law enforcement officers stationed on the bridge are expected to have higher exposure to TRAPs. The median in-vehicle ultrafine particulate (UFP) concentration at the San Ysidro POE was reported to be 45 percent higher than that observed in the same vehicles commuting on a U.S. highway, although black carbon (BC) concentrations were reported to be significantly lower in the same vehicles (Quintana et al., 2018). Nevertheless, prolonged wait time at the POE contributes to approximately 50 percent of a cross-border commuter's exposure to air pollution inside the vehicle during a 35 km commute between Tijuana and San Diego via the San Ysidro POE (Quintana et al., 2018). Pedestrians crossing the POE are also reported to have excessive exposure to the TRAPs. Pedestrians who spent an average of 60-minute wait time in the pedestrian lane would experience a twofold increase in the 24-hr averaged personal $PM_{2.5}$ exposure versus non-border commuters and a three- to sixfold increase for other gaseous pollutants at the San Ysidro POE (Galaviz et al., 2014). However, a daytime (6 a.m.–5 p.m.) weekday (M–F) average $PM_{2.5}$ concentration at a fixed location near the pedestrian pathway on the San Ysidro POE was reported to be 24±28 $\mu g/m^3$ (Mean±SD), which was not significantly higher than the 24-hr averaged exposure concentration of 21±11 $\mu g/m^3$ in the community, if the exposure concentration for non-border commuters could represent the averaged community exposure at San Ysidro. The mean value for the 24-hr averaged concentration is consistent with an averaged $PM_{2.5}$ concentration (over 21 individual days in 2010) of 19 $\mu g/m^3$ observed at a location approximately 0.4 km from this POE in San Ysidro (Quintana et al., 2014).

The impacts of TRAPs and regional industrial pollution on the health of community residents are of particular concern for the border cities of the Paso del Norte (PdN,) a region comprised of the cities of El Paso, Texas; Cd. Juárez, Chihuahua, Mexico; and Sunland Park, New Mexico. The rapidly worsening air quality along the U.S.–Mexico border is partly due to high rates of urbanization and industrial development compounded by rapid cross-border economic growth, a poorly maintained vehicle fleet, complex terrain features, and semi-arid weather (Li et al., 2001; Raysoni et al., 2017, 2011; Zora et al., 2013). Various studies have suggested that exposure to TRAPs may be associated with an increased risk of asthma and other reduced lung function ailments in schoolchildren (Branco et al., 2014; Janssen et al., 2001; Kim et al., 2016). Emissions from the four POEs in El Paso have been viewed as a major source of emissions in the community, especially for the substantial number of people living in close vicinity of the international POEs. Among the four POEs in El Paso, The Bridge of the Americas (BOTA)

has the highest traffic volume in El Paso, Texas, primarily because it is the only free POE between the U.S. and Mexico. In 2021, 3.3 million northbound vehicles crossed from Cd. Juarez to El Paso, as well as over 600,000 pedestrians crossing on foot (U.S. Customs and Border Protection, 2022). Prolonged delays of idling commercial and passenger vehicles are common at the BOTA. Excessive emissions during border crossings have also increased in recent years as a result of the aging vehicle fleet, unregulated vehicle emission inspection, heightened security, and staff shortages due to COVID-19. Delays in public transportation at the U.S.-Mexico border have been criticized for causing economic losses and exacerbating social stressors (Quintana et al., 2015). The BOTA queue can be as long as 1 km, and standard gas-powered vehicles can use up to 0.13 gal due to frequent starting and stopping. Excessive emissions from heavy-duty commercial diesel vehicles, estimated at a volume of 180,000 in 2021 (U.S. Customs and Border Protection, 2022), crossing the BOTA are higher than standard passenger cars when the vehicles are in a queue (Tong et al., 2000).

Measurements of TRAPs on the BOTA have not been conducted due to concerns about space availability and interference with bridge traffic and security protocols, although a few air quality studies were performed near the BOTA. Chen et al. (2012) measured $PM_{2.5}$ concentrations at a location approximately 0.3 km from the BOTA and reported a low three-day average $PM_{2.5}$ concentration of 8.3 $\mu g/m^3$, compared to 7.4 $\mu g/m^3$ observed at a nearby state-operated air monitoring station (CAMS 41) during a short-term intensive observing period for a potential winter PM episode (Chen et al., 2012). Olvera et al. (2013, 2011) conducted PM mass and number concentration measurements at a location in close proximity to the southbound lanes of the BOTA. The seasonal two-week measurements revealed that $PM_{2.5}$ varied insignificantly with respect to the change of season or wind direction, while the ultrafine particle (UFP) number concentrations were highest when winds were coming from the east or north (i.e., downwind) of the BOTA inspection booths. The mean $PM_{2.5}$ concentrations observed at this near-road location were higher than those observed at the nearby CAMS 41 station by approximately 50 percent (11.3±8.5 versus 7.6±5.7 $\mu g/m^3$). Hourly average UFP number concentrations ranged between $1.7x10^3$/cc and $2.9x10^5$/cc with a mean of $3.5x10^4$/cc; these values are comparably higher than what would be observed near high traffic density highways.

Traffic moving to and from the BOTA affects communities living near the BOTA. In cities with high levels of human activities around transportation corridors, there is a high incidence of health problems in the community (Cyrys et al., 2003; Sharma et al., 2009). Long-term exposure to TRAPs emissions has been shown to produce various adverse health issues (Baldauf et al., 2008; HEI, 2010). In particular, a community around Zavala Elementary School, around 0.7 km away from the BOTA, is concerned with the air pollution exposure they receive from the bridge and the possible adverse health impacts it could cause to them and their children attending the local elementary school.

This study is concerned with the potential air pollution exposure for bridge users (i.e., pedestrians, commuters, and commercial truck drivers), POE workers (i.e., U.S. Customs and Border Protection [CBP] agents, federal law enforcement workers), and residents of nearby communities. This study attempts to address the transportation-related emissions impacts on these individuals by collecting and analyzing exposure data for bridge users and POE workers. Emission impacts on the nearby communities are also addressed by analyzing the data collected using a network of low-cost air sensors. This study aims to provide community air pollution strategies to improve the air quality at the BOTA and the nearby community. To the best of our knowledge, no similar in-traffic air pollution studies have been conducted at a POE. Our results do not apply to in-vehicle exposure.

This study has three major objectives: (1) assess the levels of three major transportation-related air pollutants ($PM_{2.5}$, NO_2, and O_3) generated by vehicles passing through the POE in El Paso, Texas; (2) establish PM levels for the surrounding communities near a POE, on both sides of the border, using low-cost sensors; and (3) assess the predicted levels of PM associated with transportation-related air pollutant emissions ($PM_{2.5}$, PM_{10}, NO_2, and O_3) from the POE and the extent of exposure on the adjoining areas.

Methodology

Study Design and Site Selection

This study was conducted in El Paso, Texas, at the BOTA, and the study area chosen for this project included the BOTA POE and several sites within the city, which measured pollutant concentrations during the study period.

The air sampling campaign was conducted at the BOTA for 34 days between February 7 and March 12, 2022. Figure 1a shows the satellite image of the passenger lanes of the BOTA. Commercial trucks and passenger vehicles are directed into two separate inspection facilities at the BOTA. The commuter lanes for passenger vehicles operate 24 hours a day, seven days a week, while the commercial lanes for trucks (not shown in the figure) operate from 6:00 a.m.–4:00 p.m., Monday–Friday. Two sets of instruments were placed at the BOTA, one in the center island among the car lanes (designated Station A, Figure 1b) and the other set on an adjacent island (Station B, Figure 1c). The stations are among Ready Lanes, lanes for people who have their paperwork processed already and help cars move along quicker.

Figure 1. BOTA air pollution collection stations (a) overhead view, (b) Station A, and (c) Station B.

Additional $PM_{2.5}$ monitoring using low-cost PM sensors was conducted at locations in the vicinity of the BOTA to assess community PM exposure during the study period. A total of six units of Purple Air sensors were installed at four locations on February 18, 2022, in El Paso, while another two units were installed at one location later in Cd. Juarez (CJ5-H) on March 3, 2022, due to an unexpected delay in equipment transfer from one jurisdiction to another. Five locations were selected to create a PM monitoring network surrounding the BOTA. The four locations in El Paso were elementary schools near the BOTA at Douglass, Bowie, Zavala, and Cooley. At the Douglass, Zavala, and Bowie locations, two collocated Purple Air sensors were included for quality assurance. One of the Bowie sensors was found to be defective and was removed from this study. In Cd. Juárez, Chihuahua, two sensors were installed at the Universidad Autónoma de Cd. Juárez; this location is designated as CJ5-H.

Figure 2 shows a map of where all the Purple Air sensors were set up, as well as the location of the BOTA and a reference Texas Commission on Environmental Quality (TCEQ) CAMS 41 station. Table 1 summarizes each sensor's location and distance to the BOTA, including the locations with duplicate samples. CAMS 41 is a continuous ambient monitoring station operated by TCEQ that measures a number of pollutants, nutrients, or other parameters in the atmosphere. It is located in the Chamizal National Memorial Park (31.7656923, −106.4552321), approximately 60 m away from the Cesar Chavez Memorial Highway (Highway 375).

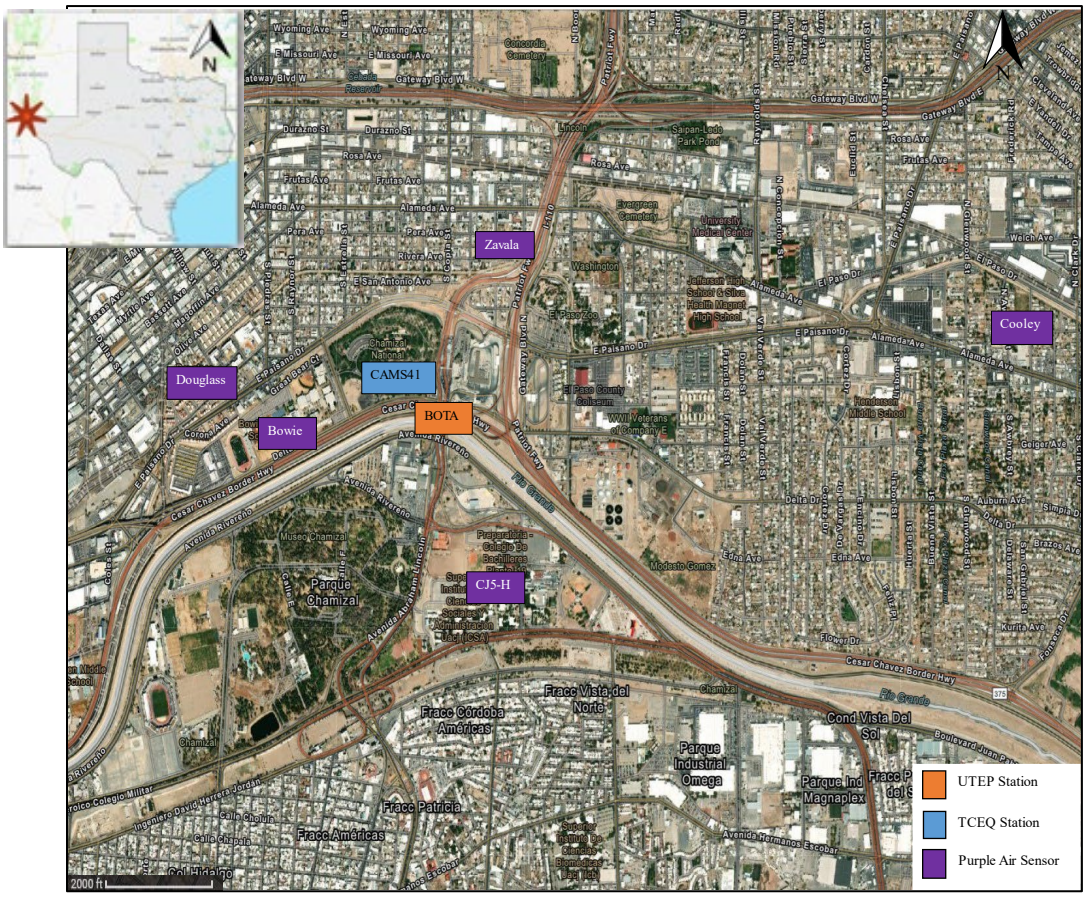

Figure 2. Map of air pollution collection sites.

Table 1. Summary of Purple Air Locations.

Name	Latitude (Degrees)	Longitude (Degrees)	Distance to BOTA (km)	Land Use Category	Number of Purple Air Sensors
Cooley	31.768	−106.417	3.2	Education Institution	1
Douglass	31.768	−106.466	1.4	Education Institution	2
Zavala	31.772	−106.447	0.7	Education Institution	2
Bowie	31.764	−106.460	0.9	Education Institution	1
CJ5-H	31.578	−106.449	1	Education Institution	2

Instrumentation and Correction

Three TRAPs ($PM_{2.5}$, O_3, and NO_2) were continuously measured at two locations on the BOTA. $PM_{2.5}$ concentrations were measured using a GRIMM 11A Portable Laser Aerosol Spectrometer and Dust Monitor (GRIMM, 2010). O_3 and NO_2 were monitored with 2B Technologies devices, Model 202 for O_3 and Model 405 for NO_2 (2B Technologies, 2017a, 2017b). One set of instruments was placed in a housing unit and connected to an external AC power. All three devices are Federal Equivalent Method (FEM) certified air monitoring instruments. Each set of instruments collected TRAP data every 5 minutes and continuously ran for the entire collection period. The instruments were protected from rain and wind by the housing unit, which also provided shade for the instruments to maintain an adequate range of operating temperature. The inlet for all instruments was set to a height of 5 ft above the ground to represent a typical breathing height for an adult. Purple Air PA-II sensors were used for community $PM_{2.5}$ monitoring. The Purple Air PA-II is an air quality sensor that measures real-time ambient and indoor $PM_{2.5}$ concentrations. It is equipped with built-in Wi-Fi capable of transmitting data to the Purple Air website, where it is stored and made available to any smart device. This low-cost sensor has been thoroughly evaluated by

the State of California's South Coast Air Quality Management District's Air Quality Sensor Performance Evaluation Center Program with acceptable precision and accuracy (http://www.aqmd.gov/aq-spec/evaluations).

Before being installed at the BOTA and Purple Air sites, all instruments were placed at another TCEQ-operated air monitoring site, CAMS 37, for two weeks for calibration against data measured by Federal Reference Method (FRM) instruments. All FEM instruments were located within 10 m of the respective FRM instruments. Displayed in Table 2 are the parameters of linear regression and the coefficients of determination between data observed between the FEM and FRM instruments. Both collocated FEM O_3 monitors performed exceptionally well against the FRM device used by TCEQ, with a slope near 1.0 and an R^2 value of 0.99. The $PM_{2.5}$ monitors also performed well against the respective FRM device but slightly overestimated the concentrations. One of the NO_2 monitors showed significant drift in the calibration, which may result in less reliable data.

Table 2. Correction Statistics against FRM Instruments for the Instruments Used at the BOTA.

Station A				Station B			
Pollutant	R^2	Slope	Intercept	Pollutant	R^2	Slope	Intercept
$PM_{2.5}$	0.80	0.81	2.09	$PM_{2.5}$	0.79	0.77	2.08
O_3	0.99	1.02	2.07	O_3	0.99	1.05	−2.12
NO_2	0.77	0.87	15.25	NO_2	0.77	0.60	1.70

Low-cost sensors could not generate data with the same quality as those monitored by FRM instruments. Therefore, the data generated by the low-cost sensors were calibrated against side-by-side data measured at a reference station using an FRM instrument. Calibration of Purple Air sensors data was conducted during late January and early February 2022. In addition, the data generated were subjected to a cleaning and quality control process according to a U.S. Environmental Protection Agency (EPA) Quality Assurance Project Plan developed from previous work. The comparative analysis was carried out with a simple linear regression analysis using the hourly averages of each sensor and the corresponding values from the reference station. The eight sensors evaluated showed a high correlation ($R2 > 0.9$) with the data measured with FRM instruments.

Data Collection

Air Pollution Monitoring at the BOTA

The instruments recorded air pollutant concentrations every 5 minutes, and the data were downloaded from the monitors once a week. Air pollution concentrations were collected for a total of 33 days. A dust storm was observed on February 21.

Meteorological Data Collection

Wind speed and direction were obtained from the reference TCEQ stations located within 0.4 km from the BOTA on a simple terrain with no abrupt elevation variations. Figure 3 displays the wind patterns at the reference site (CAMS 41) during the study period. Winds do not vary widely in the valley along the Rio Grande separating El Paso and Cd. Juarez. Westerly winds prevailed, followed by northeasterly winds during the study. Figure 3 also displays the wind roses for other TCEQ ambient air monitoring stations. It is seen in Figure 3 that westerly winds prevailed near the BOTA, and the winds gradually trended in the west-southeast direction along the Rio Grande, as seen in the wind roses for CAMS 41, 37, and 49. Surface meteorology at the BOTA is well represented by those observed at CAMS 41. Previous meteorological measurements conducted at a location adjacent to the BOTA inspection booths (shown in Figure 4 as BOTA Met) revealed that the wind patterns at the BOTA are well correlated to the measurements reported at CAMS 41, with lighter winds due to the close proximity and no noticeable terrain features between the two locations (Olvera et al., 2011). Therefore, wind measurements were not conducted at the BOTA, and data recorded at CAMS 41 were used to represent the wind conditions at the BOTA.

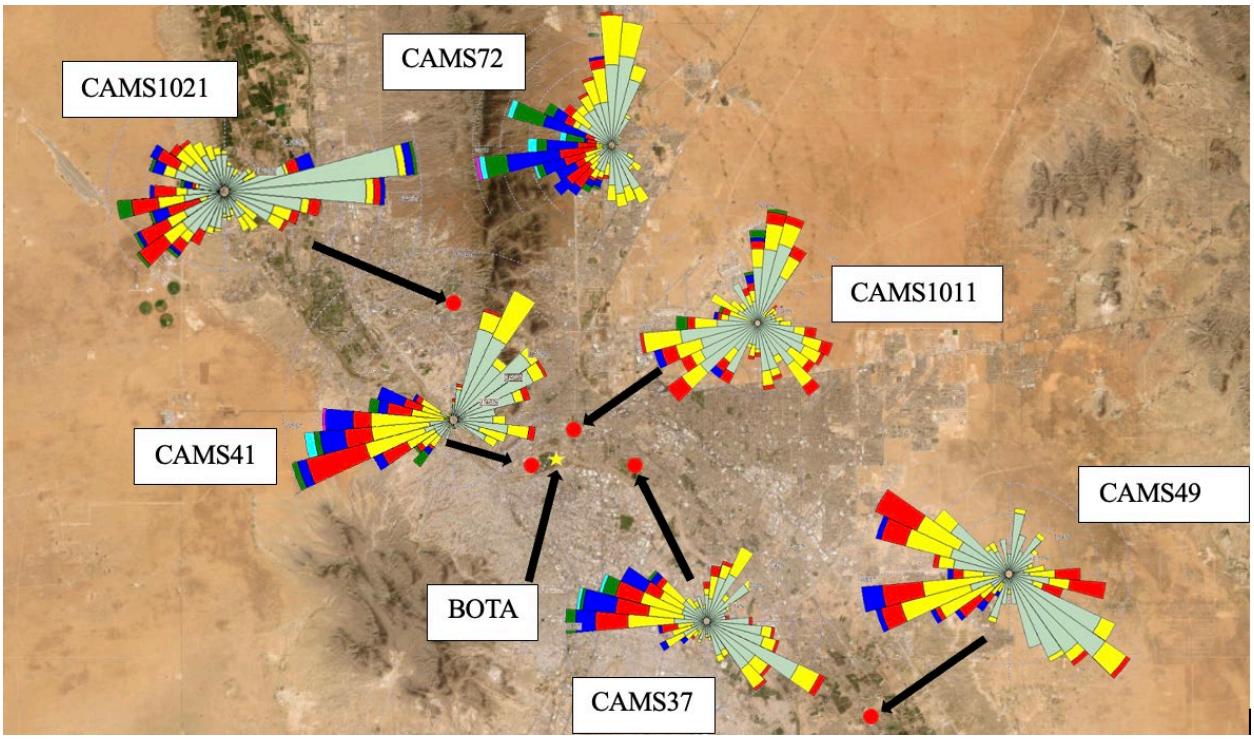

Figure 3. Wind roses at CAMS sites.

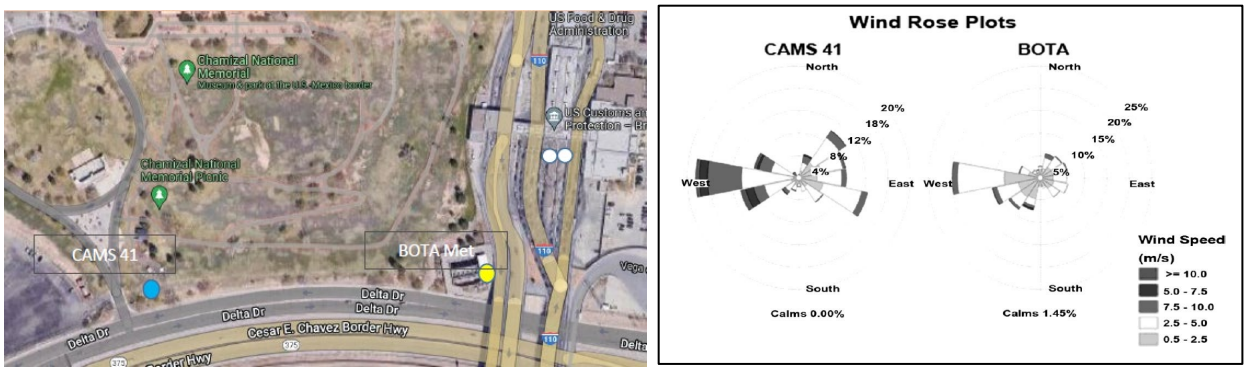

Figure 4. Similarity of wind patterns at CAMS 41 and BOTA; (a) locations of CAMS 41 and BOTA Met and (b) wind rose plots at CAMS 41 and BOTA Met (Olvera et al., 2011).

AERMOD Dispersion Modeling of BOTA Emission

The AERMOD modeling system includes the use of two regulatory components, a meteorological preprocessor (AERMET) and an air dispersion processor (AERMOD). Both hourly surface meteorological data from the El Paso International Airport, CAMS 41, and upper air soundings and minute data from the regional Santa Teresa Airport were used in AERMET to generate the on-site meteorological data for this study. The following modeling parameters and options were used in AERMOD:

- Passive pollutant.
- Volume source, characterized by 689 sources, representing the BOTA northbound lanes.
- Urban environment.
- Flat terrain.
- Ground-level release.

- Ground-level receptor.
- Initial horizontal and vertical dispersion parameters.
- Site-specific meteorology.

Microscale concentration surfaces were established and concentrations at discrete receptor locations were quantified to study the total exposures of communities near BOTA using the AERMOD air dispersion model. Pollutant air concentrations were used to apportion the contributions of emissions from the interstate highway as well as arterial roads. Figure 5 illustrates the flow of data in the AERMOD modeling process.

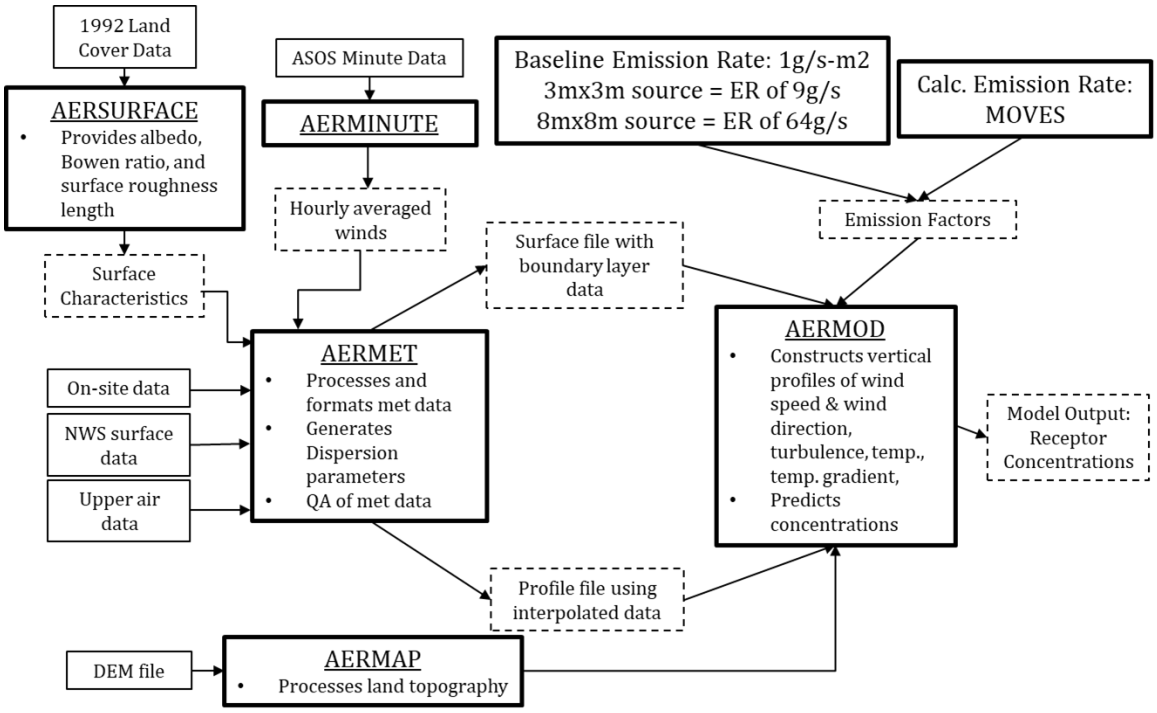

Figure 5. AERMOD model data flow.

AERMOD includes the use of two regulatory components, a meteorological preprocessor (AERMET) and a terrain data preprocessor (AERMAP). Meteorological data are needed for AERMOD modeling and refer to upper air and surface data specific to the study area monitoring station locations. Upper air data provide information to measure the characteristics that change with height in the atmosphere, such as temperature. The surface data refer to data that measure the characteristic of lower layers of the atmosphere. As shown in the data flow chart, two additional EPA regulatory processors are used to create the input files needed in AERMET. The first of these processors is AERMINUTE. A potential concern related to the use of National Weather Service (NWS) meteorological data for dispersion modeling is the often-high incidence of calms and variable wind conditions reported for the Automated Surface Observing Stations (ASOS) in use at most NWS stations. The AERMOD model currently cannot estimate dispersion under calm or missing wind conditions. To reduce the number of calms and missing winds in the surface data, AERMINUTE is used to process archived 1-minute winds for the ASOS stations to calculate hourly average wind speed and directions, which are used to supplement the standard archive of hourly observed winds processed in AERMET (U.S. EPA 2004).

In addition to raw meteorological data, AERMET requires surface characteristic information, which can be provided by processing land use data using another EPA regulatory software, AERSURFACE. When applying the AERMET meteorological processor to process meteorological data for the AERMOD model, appropriate values for three surface characteristics must be calculated: surface roughness length, albedo, and Bowen ratio. The surface roughness length is related to the height of obstacles to the wind flow and is the height at which the mean horizontal wind speed is zero based on a logarithmic profile. The surface roughness length influences the surface shear stress and is an important factor in determining the magnitude of

mechanical turbulence and the stability of the boundary layer. The albedo is the fraction of total incident solar radiation reflected by the surface back to space without absorption. The daytime Bowen ratio, an indicator of surface moisture, is the ratio of sensible heat flux to latent heat flux and, together with albedo and other meteorological observations, is used for determining planetary boundary layer parameters for convective conditions driven by the surface sensible heat flux (Cimorelli et al. 2005).

The meteorological files and emission factors established by the study parameters are used to develop a range of scenarios for dispersion modeling in AERMOD. The emission factors (EFs) are converted into a format compatible with volume source characterization in AERMOD. The BREEZE AERMOD model is commercial propriety software developed by Trinity Consultants Inc., which provides an unaltered, user-friendly, window-based version of the EPA-approved AERMOD model with pre- and post-processors and is used to help with the source and receptor coding with AERMOD. Further details regarding the processing of EFs and the AERMOD model set up are discussed in the following chapters.

AERMOD Modeling Setup

Air dispersion models such as AERMOD are used by regulatory agencies to illustrate that federally supported transportation projects will not have a significant effect on the human environment. Recognizing the important role of these models in the transportation conformity project level hot-spot process, a model-to-monitor evaluation approach is used based on hot-spot analyses. Hot-spot analysis, as defined in 40 CFR Part 93.101, is an estimation of likely future, localized pollutant concentrations and their comparison to the NAAQS. Hot-spot analyses are a part of the conformity requirements for pollutants that have localized impacts, such as particulate matter (PM). They are generally required for projects identified as being of air quality concern in the respective PM nonattainment or maintenance areas. Using this method can help maintain an adequate comparison of monitored data with modeled data. Steps to be followed in the evaluation and implementation of the modeling process are further illustrated and summarized in Table 3.

Table 3. Steps in Modeling Approach.

1. Develop 1-year of onsite meteorological data based on ambient parameters measured at the nearest continuous air monitoring stations for year 2022 combined with the nearest representative upper air and surface stations (El Paso Airport Data).
2. Set-up AERMOD with source and receptor characterization of the study area.
3. Estimate emissions rates in g/s for volume sources.
4. Calculate modeled concentrations corresponding to 1-hr maximum, 24-hr maximum, and period average.
5. Compare the modeled estimates with the monitor concentrations corresponding to 1-hr maximum, 24-hr maximum, and annual averaging period.
6. Assess the model-to-monitor comparison.

Modeling Setup

After compiling the necessary data related to meteorology, land use, and emission factors, the parameters for the dispersion modeling must be defined. Base imagery can be obtained from sources such as Google Earth, ArcMap, or the Input map feature in the BREEZE AERMOD graphic user interface.

Model Parameters

For this study, the dispersion model was set to estimate the pollutant OTHER, with no depositions and settling. Concentration estimates were calculated for hourly, maximum hour, 24-hour, and all-period (2/7–3/11) averages. AERMOD allows for two different designations for land use: urban and rural site. If at least 50 percent of the land use within a 3-km radius of the model domain is of an urban type, the source is designated urban, and rural if otherwise (U.S. EPA 2018). For urban areas, the model activates the urban heat effect, a term used to describe urban areas that are hotter than nearby rural

areas, especially at night, mainly as a result of heat retention by urban materials. Because of this heat retention, the vertical motion of the air is increased through convection, thereby leading to the increased dispersion of pollutants. AERMOD accounts for urban dispersion effects and also requires the urban area population to determine the degree of urban heat island effect occurring in a specific urban area. In this study, the modeling domain is classified as "urban."

Source Characterization and Dispersion Parameters

AERMOD can model roadway line source as a series of volume or area sources. In our study, roadway emissions are modeled as a series of volume sources.

Source Characterization

Volume sources model emissions with a uniform distribution along the roadway link and are not distributed beyond the edge of a defined roadway link. In AERMOD, a series of volume sources can model roadways and queuing links. This source characterization requires a higher number of small sources to accurately represent the roadway emissions. The combination of small volume sources represents in detail the physical dimensions and orientation of the roadway links. Figure 6 shows the base configuration of the 690 volume sources used in this model. This is a combination of 587 3-m × 3-m and 102 8-m × 8-m wide volume sources with different vertical dimensions for representation of initial vertical dispersion, as defined in the following section.

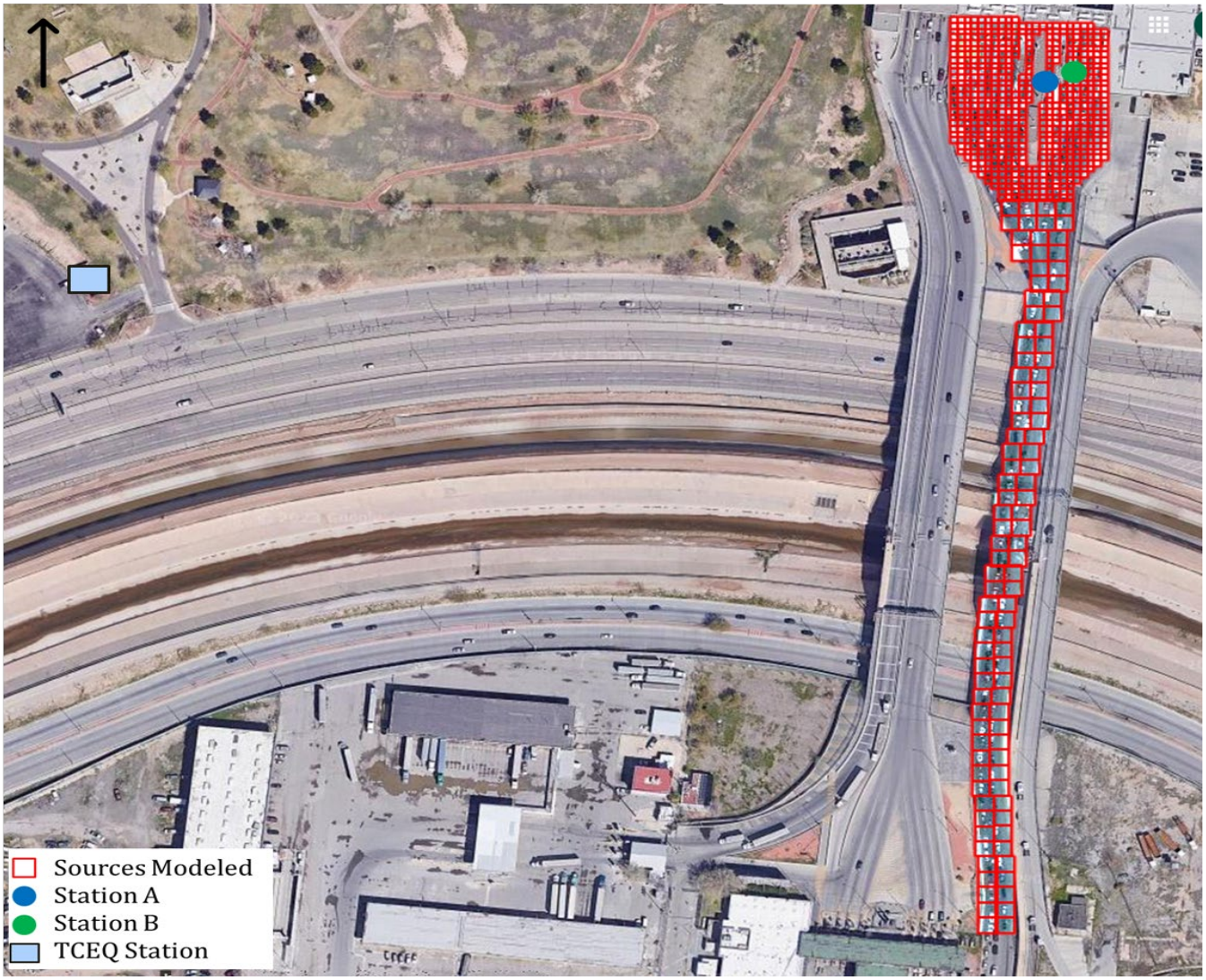

Figure 6. Volume source set-up.

Initial Dispersion Characterization

To simulate the initial dispersion on roadways due to the additional turbulent mixing of the winds behind and around the vehicle due to the physical presence of the vehicles, AERMOD allows the users to characterize the wake effect around the vehicles by defining an initial horizontal dispersion coefficient and a vertical dispersion coefficient. According to EPA hot-spot guidance, the initial vertical dimension for roadway emissions is assumed to be about 1.7 times the average vehicle height to account for the effects of vehicle-induced turbulence (U.S. EPA, 2015). For light-duty vehicles modeled in this study, this height is about 2.6 m, using an average vehicle height of 1.53 m. The AERMOD User's Guide recommends that the initial vertical dispersion coefficient (σz_o) to be estimated for a volume source by dividing the initial vertical dimension by 2.15. For typical light-duty vehicles, this value corresponds to a σz_o of 1.2 m. Initial lateral dispersion is also required for modeling volume sources and is defined as dividing the initial width of each source by 2.15; this results in 3.72 for sources with width of 8 m, and 1.395 for sources with width of 3 m.

Source Release Height

The source release height is the height at which winds begin to affect the plume. It is estimated from the midpoint of the initial vertical dimension. In this study, the source release height is calculated to be 1.3 m.

Emission Rates

Characterizing emission sources consists of defining their area and assigning the rate at which emissions are produced by the source. Emission factors for area source characterization must be input into AERMOD in units of g/sec/m^2. This study's base run assigned an EF of 1 g/s/m^2. An additional emission rates analysis was done using ERs provided by the Texas A&M Transportation Institute (TTI) for the El Paso area, which were created for the El Paso metropolitan planning organization's yearly review. This process is further described in the following section.

Receptor Selection

Receptors are points at which the AERMOD model provides concentration estimates for the pollutant modeled. Receptors for the study area were placed at an elevation equal to the meteorological site (i.e. ground-level) at the six discrete locations of air pollution monitors deployed during the study period. A grid of around 3,000 receptors was also placed to capture concentration estimates throughout the entire study area. Figure 7 shows the model set-up with the 690 sources and the grid and discrete receptors used for creating concentration surface maps.

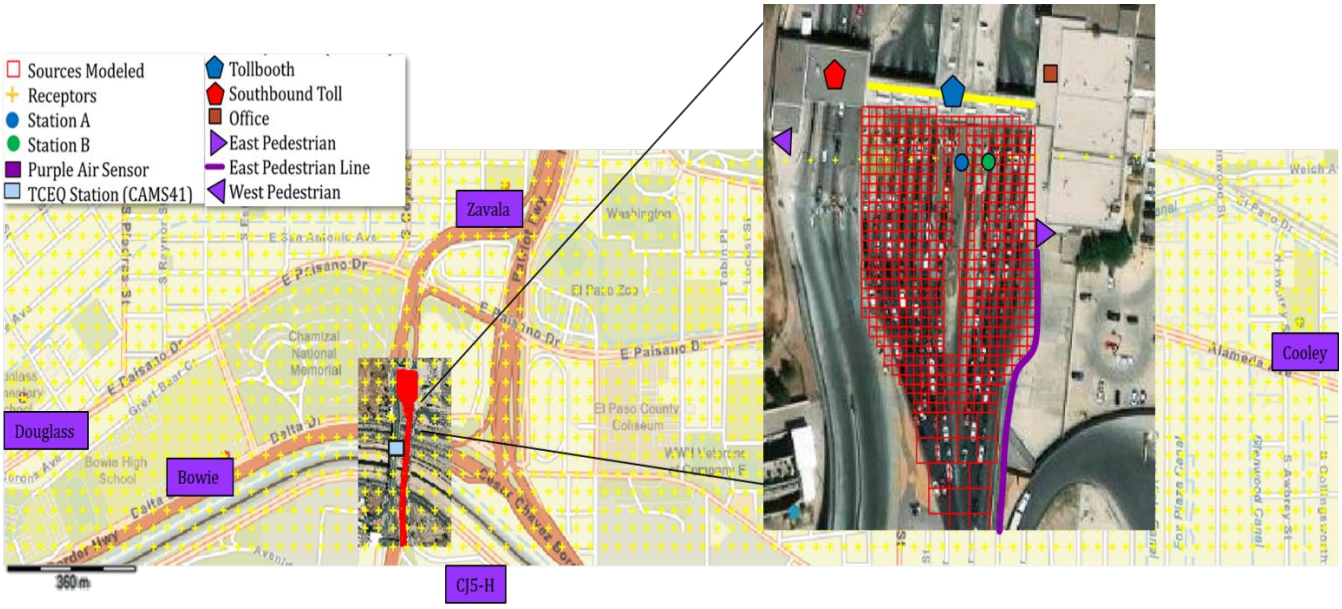

Figure 7. AERMOD area source and receptor model set-up.

Modeling Scenarios

Queue Length Analysis

In order to test the impact of queue length (the size of the volume source represented in the model or wait time on the BOTA) on exposure, multiple analyses were done reducing the length of the queue by reducing the number of sources. All input parameters remained the same, and only the number of sources was reduced, as detailed in

Table 4, with Scenario 1 being the base run of length 480 m with 100 percent of all volume sources modeled. The map configuration of the different lengths of the queue are shown in Figure 8.

Table 4. Queue Length Analysis Scenario Descriptions.

Scenario Number	Queue Length (m)	Number of Sources	% of $(3m)^2$ Sources	% of $(8m)^2$ Sources
Scenario 1	480	690	100	100
Scenario 2	370	662	100	75
Scenario 3	270	637	100	50
Scenario 4	165	611	100	25
Scenario 5	90	587	100	0
Scenario 6	70	450	75	0
Scenario 7	45	293	50	0
Scenario 8	24	147	25	0

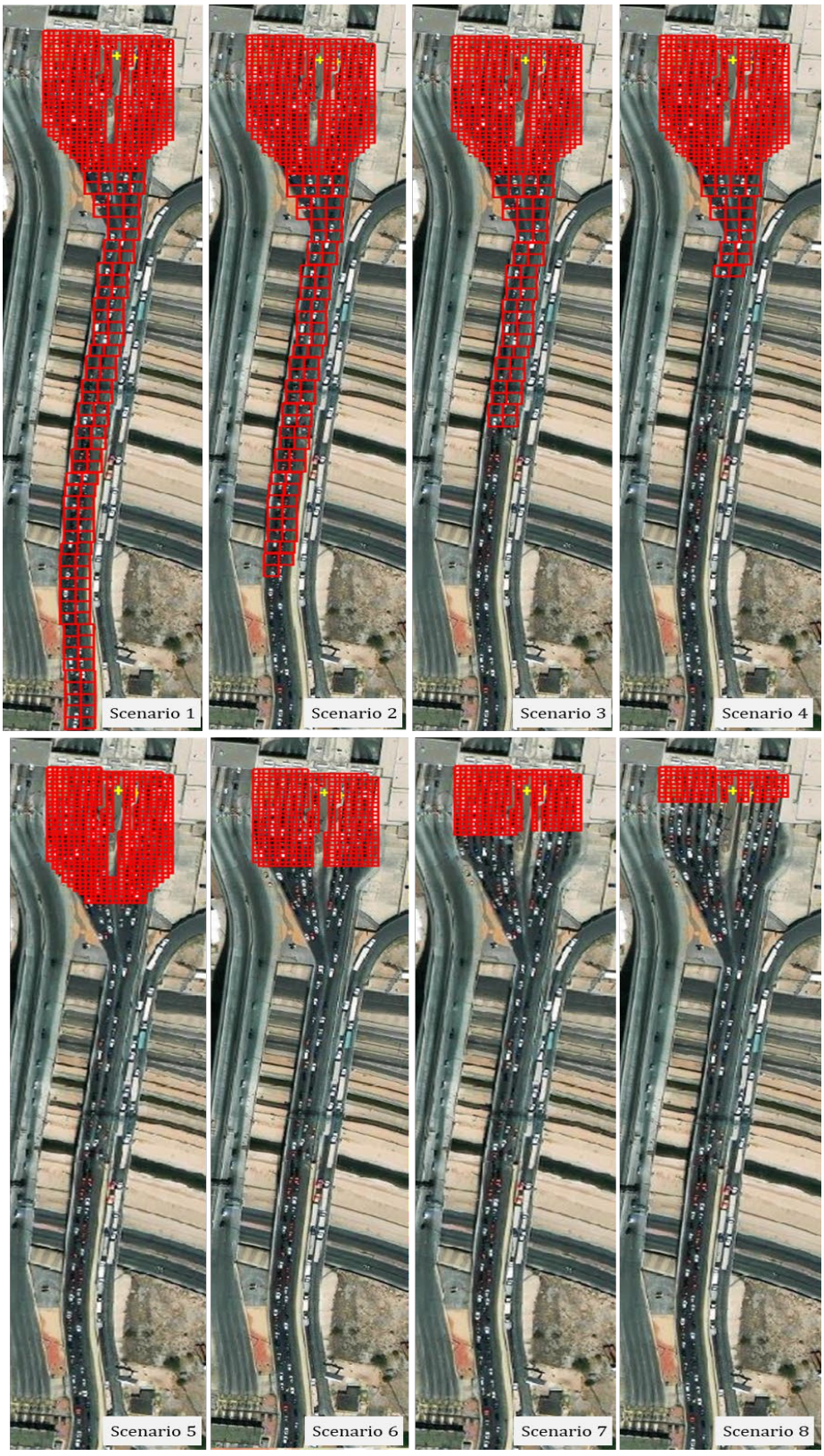

Figure 8. Queue length analysis.

Emissions Rates Calculations and Analysis

TTI published and developed a report on the development of emissions rate lookup tables (ERLTs) (Texas A&M Transportation Institute, 2022). This study computes the ERLTs for criteria air pollutants (CAP), mobile source air toxics (MSAT), and greenhouse gases. CAP and MSAT pollutants are regulated under the Clean Air Act (CAA) and need to be incorporated in various air quality assessments. The ERLTs provided emissions rates for TxDOT districts, including the El Paso District, for running emission rates (g/mi) by average speed and road type, idling emission rates (g/hr) by road type, start emission rates (g/start) by vehicle and fuel type combination, and extended idling emission rates (g/hr) for combination long-haul trucks. Additionally, each analysis included representation for winter, spring, summer, and fall seasons. Therefore, this study obtained the emissions rates for the El Paso District for the winter season using running emissions rates in g/mi on arterial road types for average speeds of 2.5 mph. The average speeds of 2.5 mph were used to represent the "stop and go" scenario for vehicles crossing at the POE. Winter rates for urban arterial roads at an average speed of 2.5 mph per distance in g/mi were converted into the appropriate units to be used in AERMOD, g/s-m^2. The base ERs used for three different criteria pollutants studied in this project are shown in Table 5. Modeled concentration estimates for $PM_{2.5}$ and PM_{10} are presented in ($\mu g/m^3$), and modeled concentrations for NO_2 are converted and presented in ppb.

Table 5. Running Emissions Rates for Winter Season at 2.5 mph.

Unit	$PM_{2.5}$	PM_{10}	NO_2
g/mile	0.058	0.373	0.033
g/veh-hr	0.145	0.933	0.083
g/veh-s	4.03E-05	2.59E-04	2.31E-05
g/s-m2	1.92E-06	1.23E-05	1.10E-06

In addition, historical average wait times for February and March from the CBP database were obtained for every hour and every day of the week (U.S. Customs and Border Protection, 2022). Figure 9 shows the average hourly wait times, in minutes, for days of the week during February–March, including the weekend and weekday averages.

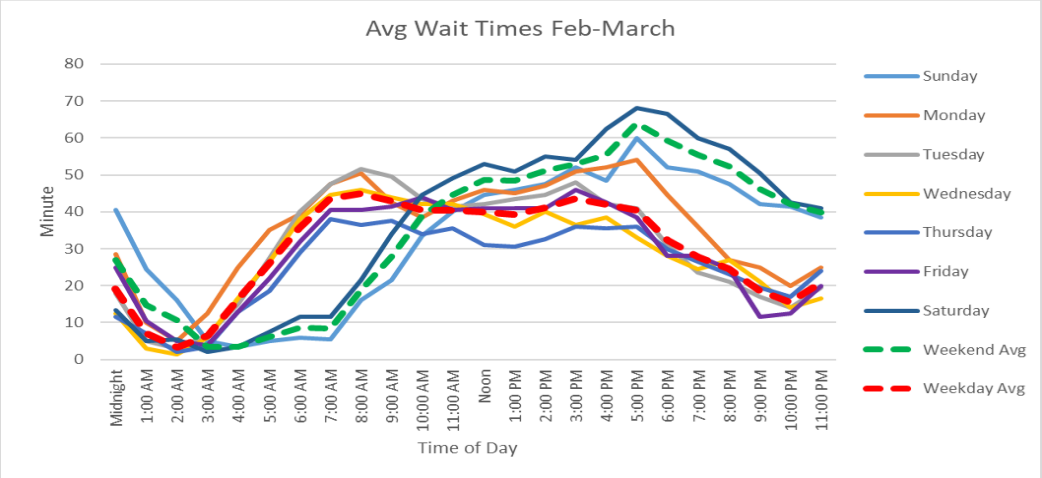

Figure 9. Average wait times for February and March at the BOTA.

It is seen in

Figure 9 that wait times follow similar patterns to expected traffic volume; that is, the weekday average shows a peak in wait time at 7 a.m. and another around 4 p.m. During the average weekend, wait times start to increase at 10 a.m. and continue rising throughout the day, peaking at 6 p.m. These hourly wait times were then used to normalize the winter ERs to create an hourly ER for an average weekday and weekend. The following equations describe the process carried out to create these hourly ERs:

$$ER_{hr} = ER_{winter} \times \frac{WT_{hr}}{WT_{avg}} \quad (1)$$

Adj. ER_{hr}: Adjusted emission rate for weekend or weekday hour in g/s;
ER_{winter}: Emission rate for winter in g/s;
WT_{hr}: Wait time per hour in minutes; and
WT_{avg} : Average Wait time for weekend or weekday in minutes

Once the hourly ERs were calculated for weekday and weekends in g/s, they were converted to g/s-m^2 depending on the area of the volume source. Table 6 shows the hourly weekend and weekday ERs by pollutant and source size; volume sources were either 9m^2 or 64m^2. These ERs were used to create an "HRLY" file for use with the AERMOD model, which also incorporates the initial lateral dispersion and initial vertical dispersion previously mentioned. These emissions do not reflect the queue length but rather the varying time emissions rates experienced on the roadway of the POE.

Table 6. Emissions Rates by Source Area Size, Weekday/Weekend, and Pollutant.

Source Size	$PM_{2.5}$				PM_{10}				NO_2			
	9m^2		64m^2		9m^2		64m^2		9m^2		64m^2	
Time	Weekend	Weekday	Weekend	Weekday	Weekend	Weekday	Weekend	Weekday	Weekend	Weekday	Weekend	Weekday
Midnight	1.3E-05	1.1E-05	9.6E-05	7.9E-05	8.69E-05	7.15E-05	6.18E-04	5.08E-04	7.75E-06	6.37E-06	5.51E-05	4.53E-05
1:00 AM	7.4E-06	4.1E-06	5.2E-05	2.9E-05	4.75E-05	2.66E-05	3.37E-04	1.89E-04	4.23E-06	2.37E-06	3.01E-05	1.68E-05
2:00 AM	5.4E-06	1.9E-06	3.8E-05	1.4E-05	3.46E-05	1.24E-05	2.46E-04	8.78E-05	3.08E-06	1.10E-06	2.19E-05	7.83E-06
3:00 AM	1.7E-06	3.8E-06	1.2E-05	2.7E-05	1.13E-05	2.43E-05	8.01E-05	1.73E-04	1.00E-06	2.17E-06	7.14E-06	1.54E-05
4:00 AM	1.7E-06	9.6E-06	1.2E-05	6.8E-05	1.13E-05	6.18E-05	8.01E-05	4.39E-04	1.00E-06	5.51E-06	7.14E-06	3.92E-05
5:00 AM	3.1E-06	1.5E-05	2.2E-05	1.1E-04	2.01E-05	9.69E-05	1.43E-04	6.89E-04	1.79E-06	8.64E-06	1.27E-05	6.15E-05
6:00 AM	4.4E-06	2.1E-05	3.1E-05	1.5E-04	2.81E-05	1.34E-04	2.00E-04	9.50E-04	2.51E-06	1.19E-05	1.78E-05	8.47E-05
7:00 AM	4.2E-06	2.5E-05	3.0E-05	1.8E-04	2.73E-05	1.63E-04	1.94E-04	1.16E-03	2.44E-06	1.46E-05	1.73E-05	1.03E-04
8:00 AM	9.4E-06	2.6E-05	6.7E-05	1.9E-04	6.03E-05	1.68E-04	4.29E-04	1.20E-03	5.38E-06	1.50E-05	3.82E-05	1.07E-04
9:00 AM	1.4E-05	2.5E-05	9.9E-05	1.8E-04	8.93E-05	1.61E-04	6.35E-04	1.14E-03	7.96E-06	1.44E-05	5.66E-05	1.02E-04
10:00 AM	1.9E-05	2.3E-05	1.4E-04	1.7E-04	1.25E-04	1.51E-04	8.92E-04	1.08E-03	1.12E-05	1.35E-05	7.96E-05	9.59E-05
11:00 AM	2.2E-05	2.4E-05	1.6E-04	1.7E-04	1.43E-04	1.52E-04	1.02E-03	1.08E-03	1.28E-05	1.35E-05	9.08E-05	9.61E-05
Noon	2.4E-05	2.3E-05	1.7E-04	1.6E-04	1.57E-04	1.49E-04	1.12E-03	1.06E-03	1.40E-05	1.33E-05	9.94E-05	9.47E-05
1:00 PM	2.4E-05	2.3E-05	1.7E-04	1.6E-04	1.56E-04	1.47E-04	1.11E-03	1.04E-03	1.39E-05	1.31E-05	9.89E-05	9.30E-05
2:00 PM	2.6E-05	2.4E-05	1.8E-04	1.7E-04	1.65E-04	1.53E-04	1.17E-03	1.09E-03	1.47E-05	1.37E-05	1.05E-04	9.73E-05
3:00 PM	2.6E-05	2.5E-05	1.9E-04	1.8E-04	1.71E-04	1.63E-04	1.21E-03	1.16E-03	1.52E-05	1.45E-05	1.08E-04	1.03E-04
4:00 PM	2.8E-05	2.4E-05	2.0E-04	1.7E-04	1.79E-04	1.58E-04	1.27E-03	1.12E-03	1.59E-05	1.40E-05	1.13E-04	9.99E-05
5:00 PM	3.2E-05	2.4E-05	2.3E-04	1.7E-04	2.06E-04	1.52E-04	1.46E-03	1.08E-03	1.84E-05	1.35E-05	1.31E-04	9.61E-05
6:00 PM	3.0E-05	1.9E-05	2.1E-04	1.3E-04	1.91E-04	1.21E-04	1.36E-03	8.60E-04	1.70E-05	1.08E-05	1.21E-04	7.67E-05
7:00 PM	2.8E-05	1.6E-05	2.0E-04	1.1E-04	1.79E-04	1.04E-04	1.27E-03	7.37E-04	1.59E-05	9.24E-06	1.13E-04	6.57E-05
8:00 PM	2.6E-05	1.4E-05	1.9E-04	1.0E-04	1.68E-04	9.17E-05	1.20E-03	6.52E-04	1.50E-05	8.18E-06	1.07E-04	5.81E-05
9:00 PM	2.3E-05	1.1E-05	1.6E-04	7.8E-05	1.49E-04	7.04E-05	1.06E-03	5.00E-04	1.33E-05	6.27E-06	9.43E-05	4.46E-05
10:00 PM	2.1E-05	9.0E-06	1.5E-04	6.4E-05	1.35E-04	5.80E-05	9.61E-04	4.13E-04	1.20E-05	5.17E-06	8.57E-05	3.68E-05
11:00 PM	2.0E-05	1.2E-05	1.4E-04	8.7E-05	1.28E-04	7.85E-05	9.09E-04	5.59E-04	1.14E-05	7.00E-06	8.11E-05	4.98E-05

Results and Discussion

Analysis of BOTA Air Pollution Data

Data collected at the two BOTA stations were compared to each other. Figure 10 shows the scatter plots of $PM_{2.5}$, O_3, and NO_2 at the two locations. $PM_{2.5}$ and O_3 data between the two stations (Figure 10a and Figure 5b) were extremely similar and strongly correlated ($R^2 > 0.98$ and slope < 1.05); as such, only the Station A data, hereinafter, are used to represent the concentrations at the BOTA for these two pollutants in the following analyses. NO_2 concentrations observed at the two relatively close locations show larger variation in Figure 10c, although they are still well correlated. NO_2 is a product of combustion and an EPA criteria pollutant primarily emitted from vehicle exhausts and industrial sources. NO_2 is rapidly depleted in the atmosphere during the day, especially under strong solar radiation, and is a precursor for O_3 formation. NO_2 begins to accumulate after sunset when the O_3-NO_2 photolysis ceases to function. The rapid, complex chemical reactions between NO-NO_2-O_3 near the vehicle exhaust in conjunction with local meteorological conditions may contribute to the data variability.

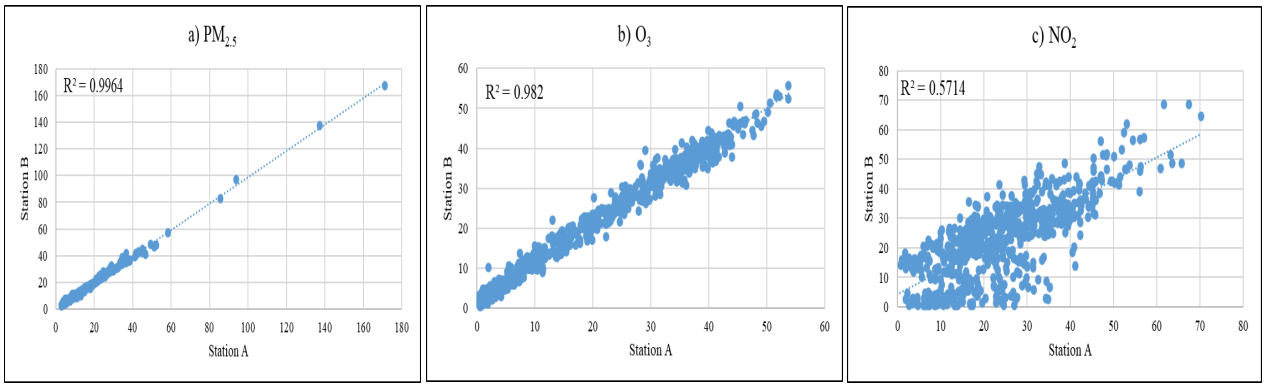

Figure 10. Pearson correlations between Stations A and B at the BOTA.

The 5-minute in-traffic data recorded at the two BOTA locations were averaged into hourly concentrations for further analysis.

Table 7 shows the descriptive statistics of the 5-minute and 1-hr average TRAP concentrations collected at the BOTA, showing average, median, standard deviation, minimum, 25th percentile, 75th percentile, and absolute maximum. Five-minute average $PM_{2.5}$ concentration occasionally peaked during the day under high wind conditions, while NO_2 peaked during possible prolonged wait time or while poorly maintained vehicles were present at the inspection booth. Nevertheless, the period averaged $PM_{2.5}$ concentrations over the length of 33 days were less than the annual NAAQS of 12 $\mu g/m^3$, while period averaged NO_2 concentration was less than the annual NAAQS of 53 ppb. The 1-hr average O_3 concentration during the study period never exceeded the 8-hr NAAQS of 70 ppb, while the hourly NO_2 concentration was always below the 1-hr NAAQS of 100 ppb. The maximum 1-hr $PM_{2.5}$ average concentration was much less than the 24-hr average NAAQS of 35 $\mu g/m^3$.

Table 7. Descriptive Statistics for TRAP Concentrations Measured at the BOTA.

5-Minute Data								
Pollutant		Average	Median	Standard Deviation	Minimum	25th Percentile	75th Percentile	Absolute Maximum
$PM_{2.5}$ ($\mu g/m^3$)	A	11.6	7.9	13.6	2.7	5.5	12.8	434.4
	B	11.6	8.0	13.4	2.6	5.6	12.9	454.0
O_3 (ppb)	A	23.7	25.9	14.2	0.0	10.2	35.7	97.0
	B	23.7	25.6	14.5	0.1	9.9	36.2	110.4
NO_2 (ppb)	A	24.9	23.9	13.5	0.0	14.9	33.9	107.0
	B	24.9	25.0	12.7	0.0	16.2	32.3	118.9
1-Hour Data								
Pollutant		Average	Median	Standard Deviation	Minimum	25th Percentile	75th Percentile	Absolute Maximum
$PM_{2.5}$ ($\mu g/m^3$)	A	11.6	8.1	11.8	2.9	5.7	13.1	171.2
	B	11.6	8.3	11.7	2.8	5.7	12.9	167.5
O_3 (ppb)	A	22.2	24.0	14.5	0.4	7.5	35.1	53.7
	B	23.3	24.8	14.2	0.5	9.5	35.8	55.7
NO_2 (ppb)	A	24.0	23.3	12.9	0.5	14.5	32.4	70.2
	B	23.1	23.7	12.9	0.5	14.2	31.5	68.7

Diurnal variations of pollutant concentrations during weekdays and weekends are displayed in

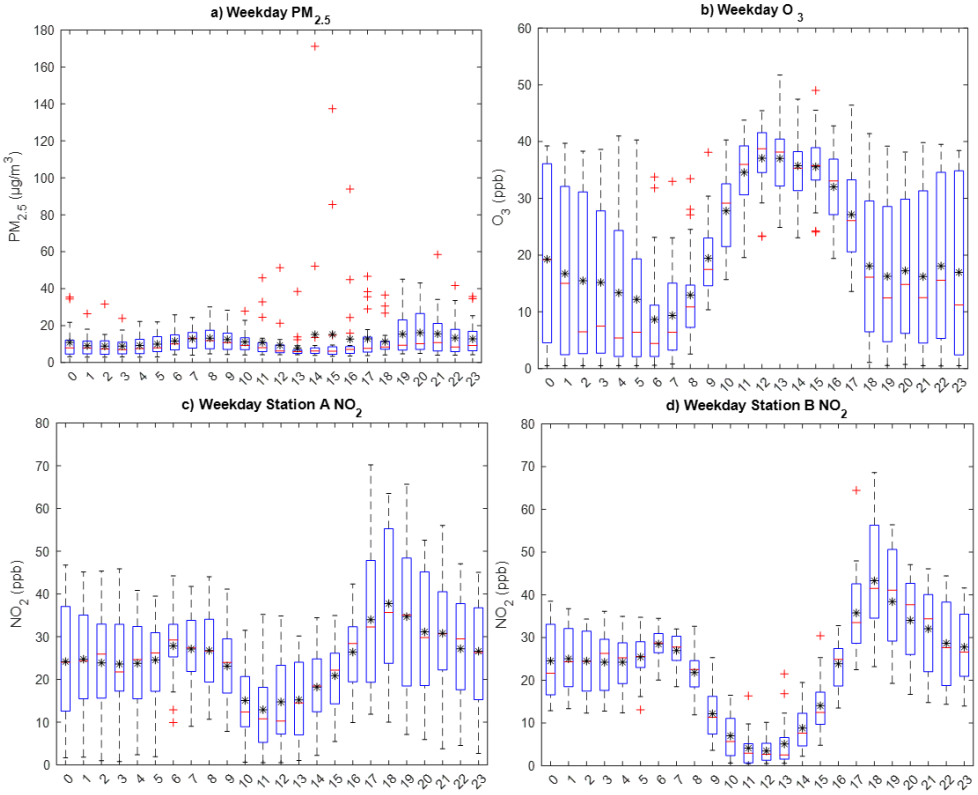

Figure 11 and

Figure 12, respectively, where the distribution of data for the hour are marked in terms minimum (Q1-1.5•IQR), first quartile (Q1), median, third quartile (Q3), and maximum (Q3+1.5•IQR). The fluctuation of concentration by hours is evident in these figures. O_3 peaks in the midday hours (10 a.m.–5 p.m.) when the temperature is hottest, while NO_2 concentrations are at their lowest in the same period. The $PM_{2.5}$ concentrations are higher during weekends (

Figure 12), as seen in the trends implied by the median and mean values of the hours, and the diurnal peaks shifted from morning traffic hours (6–9 a.m.) to noon (10–12 p.m.) and from early evening traffic hours (7–9 p.m.) to late evening (8–10 p.m.), reflecting the increased cross border economic and family activities on weekends.

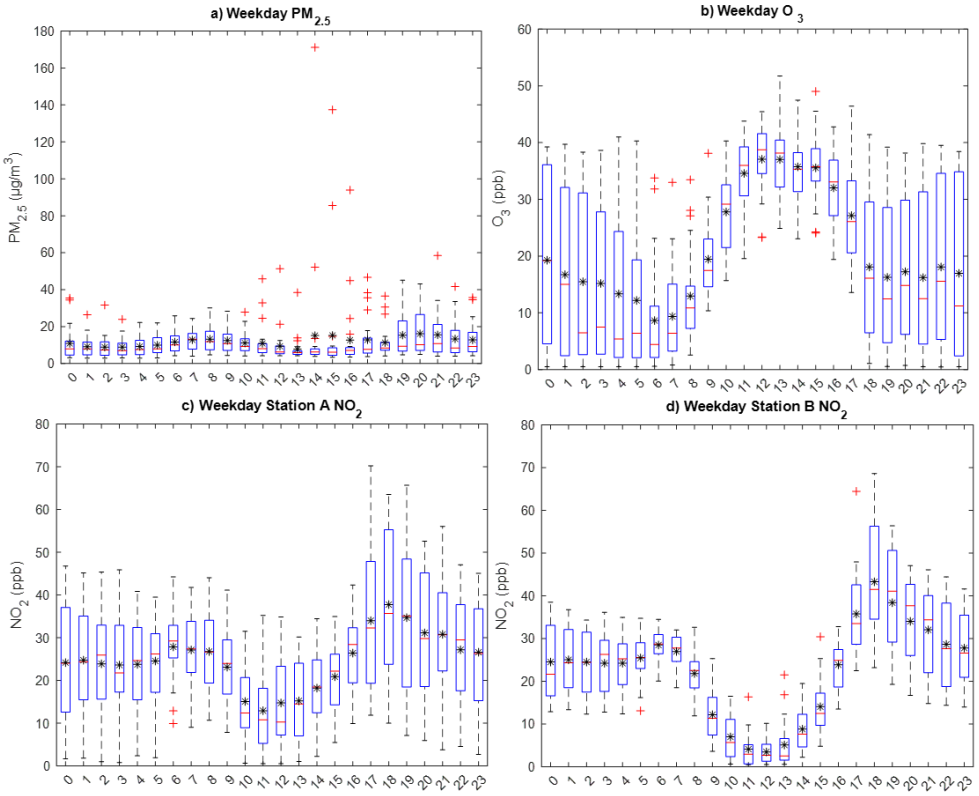

Figure 11. Weekday hourly variation of (a) $PM_{2.5}$, (b) O_3, (c) Station A NO_2, and (d) Station B NO_2 at the BOTA, where the distribution of data for the hour are marked in terms minimum (Q1-1.5•IQR), first quartile (Q1), median, third quartile (Q3), and maximum (Q3 + 1.5 IQR).

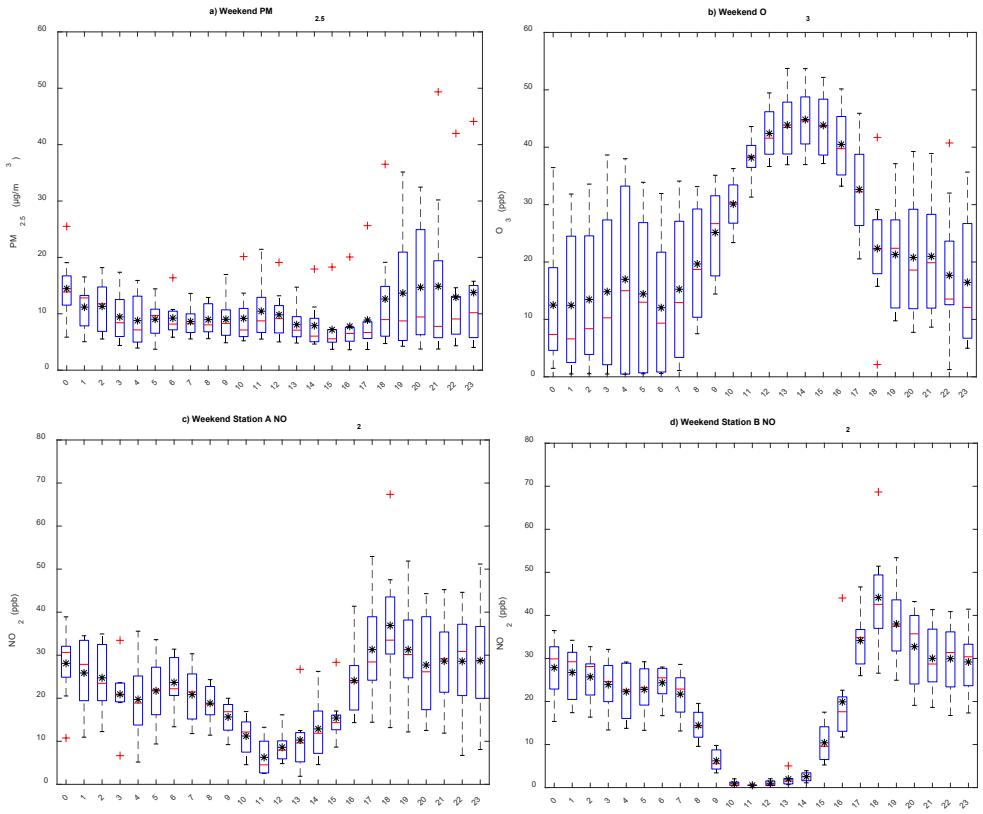

Figure 12. Weekend hourly variation of (a) $PM_{2.5}$, (b) O_3, (c) Station A NO_2, and (d) Station B NO_2 at the BOTA.

$PM_{2.5}$ Concentrations in the Community

$PM_{2.5}$ data observed in the community using the low-cost Purple Air sensors are shown in

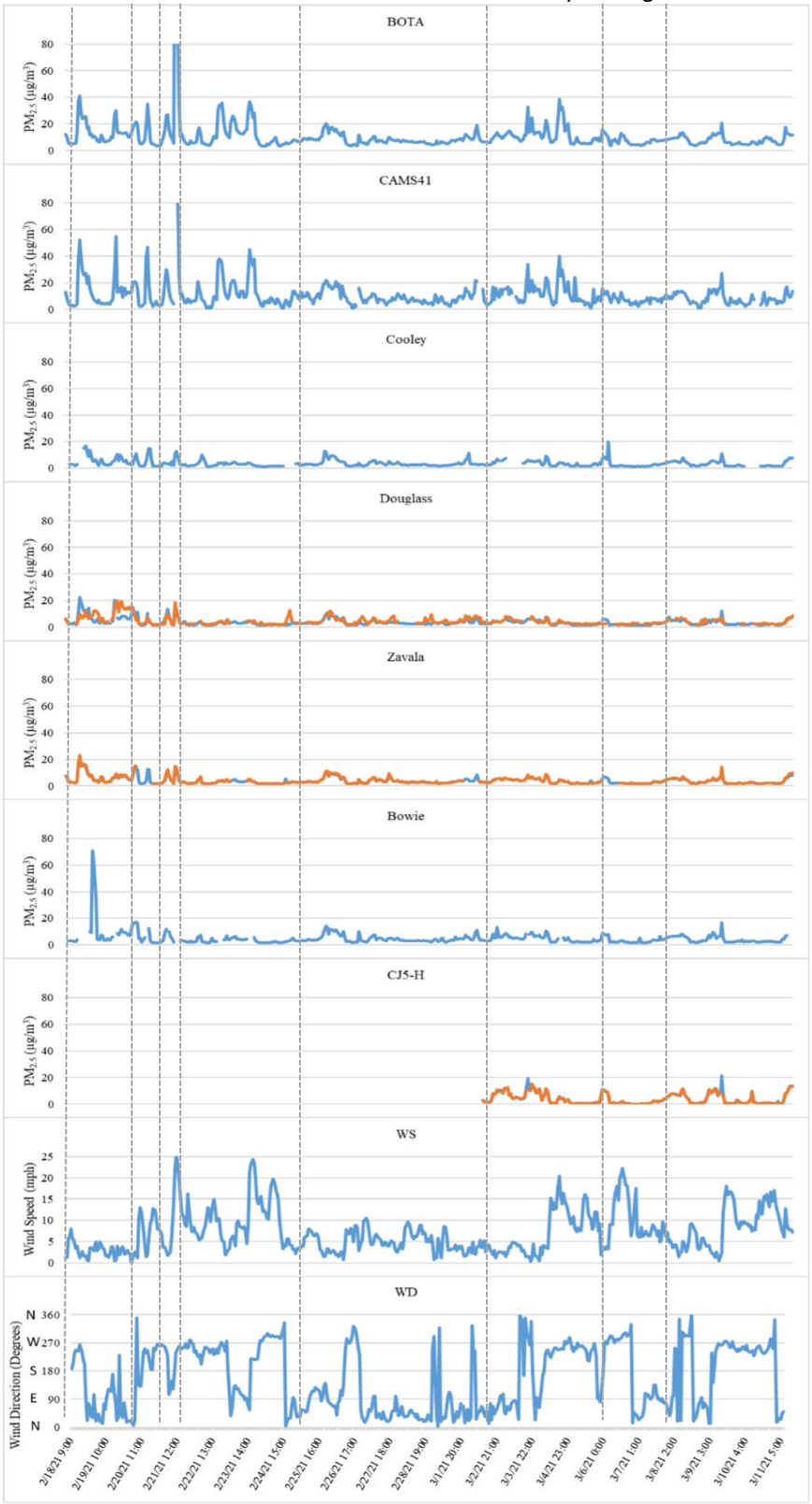

Figure 13. Collocated sensors (blue and red lines in Figure 13) at Douglass, Zavala, and CJ5-H agree well with each other, following a nearly identical trend. Concurrent data recorded at the BOTA are also shown in the figure. While Purple Air sensors might have caught the pollution trend in the occurrences of local peak $PM_{2.5}$ concentrations, as identified with dashed lines in

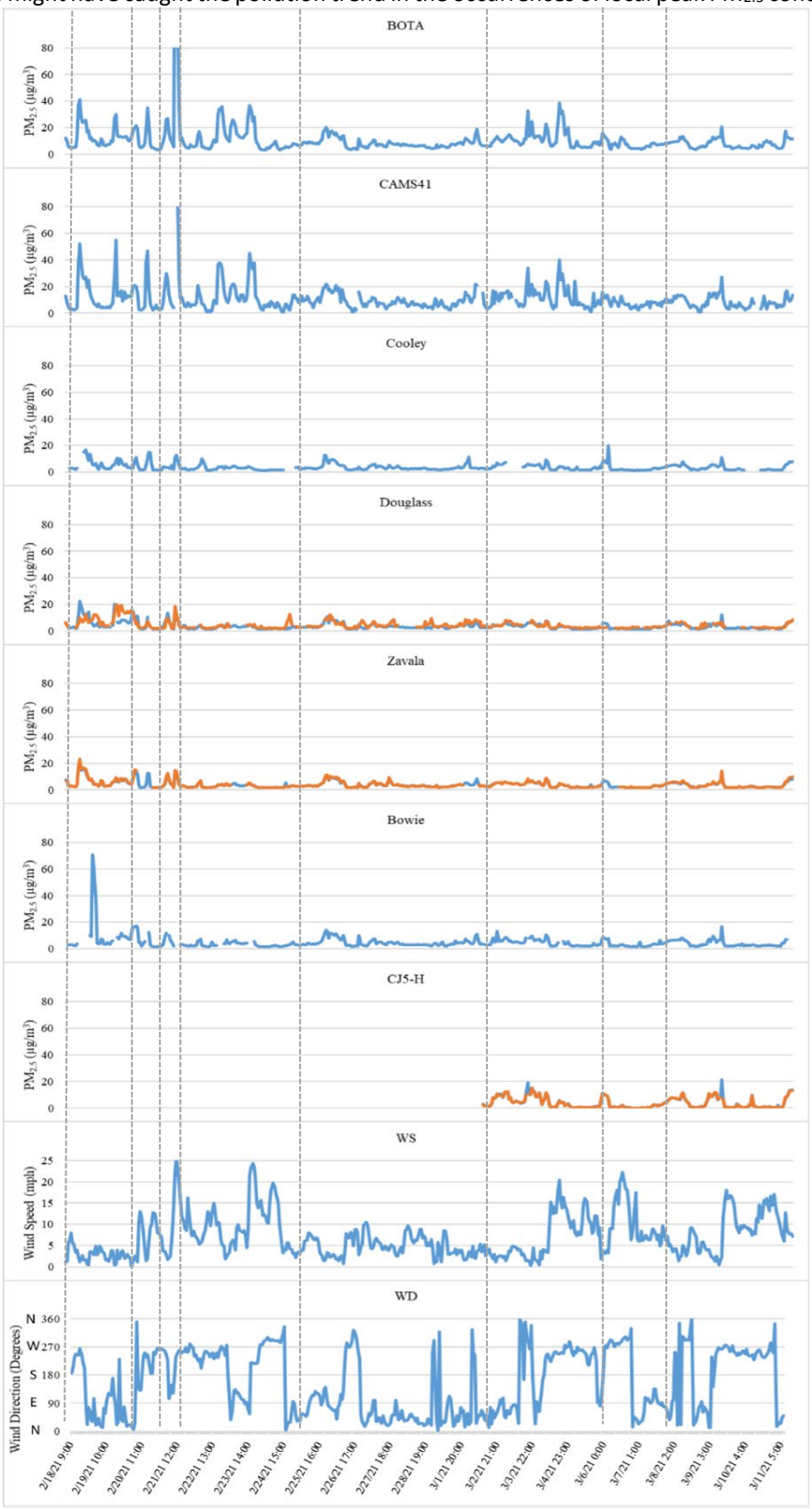

Figure 13, the $PM_{2.5}$ data observed by the low-cost sensors appeared to be significantly less than the values observed at the BOTA. The last two panels of

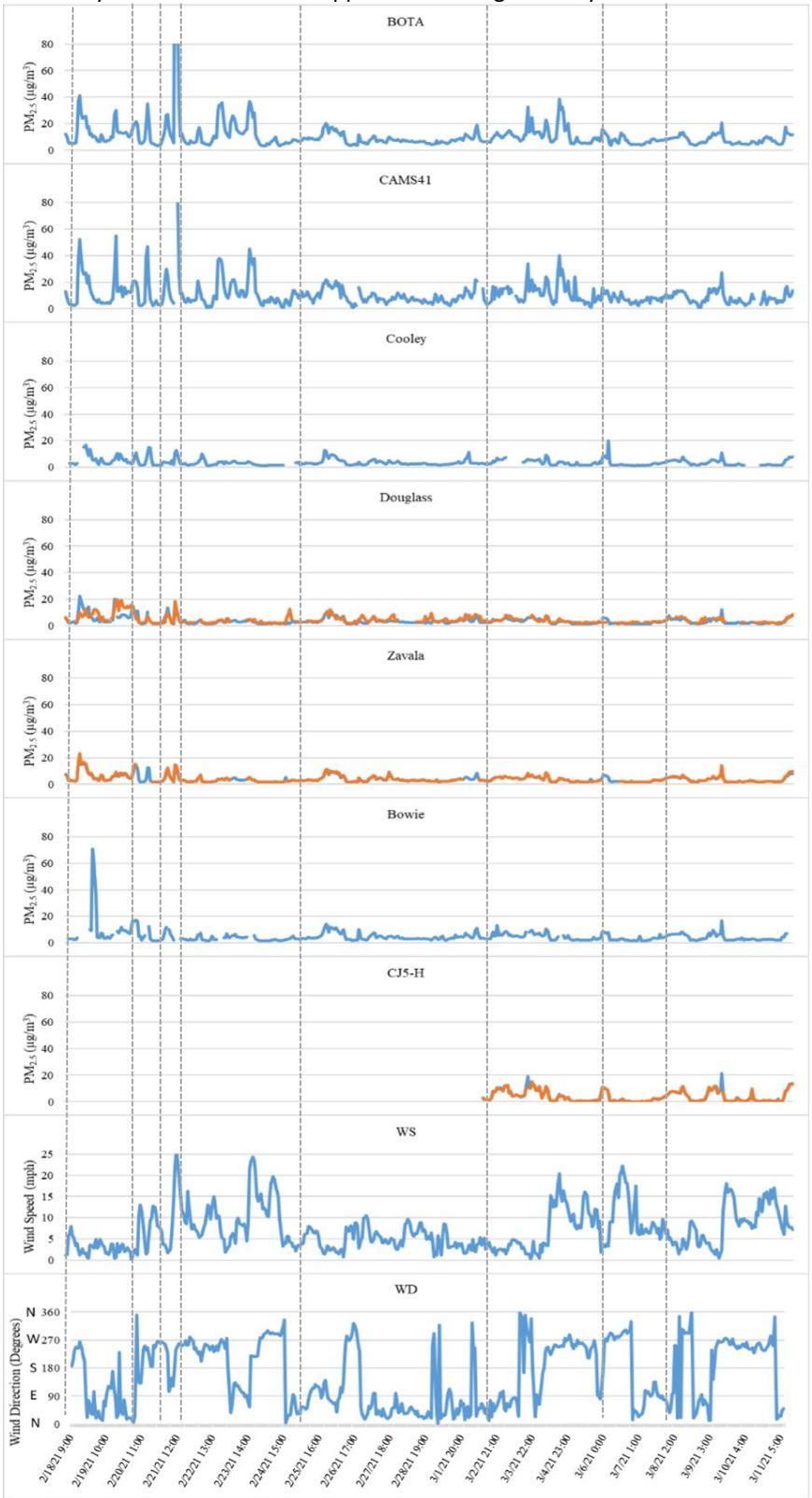

Figure 13 show the time series plots of wind direction and wind speed. Surface meteorological conditions appeared not to be a significant factor in the variability of PM concentrations in the community. Further discussion on community PM exposure is deferred to the following section in this paper.

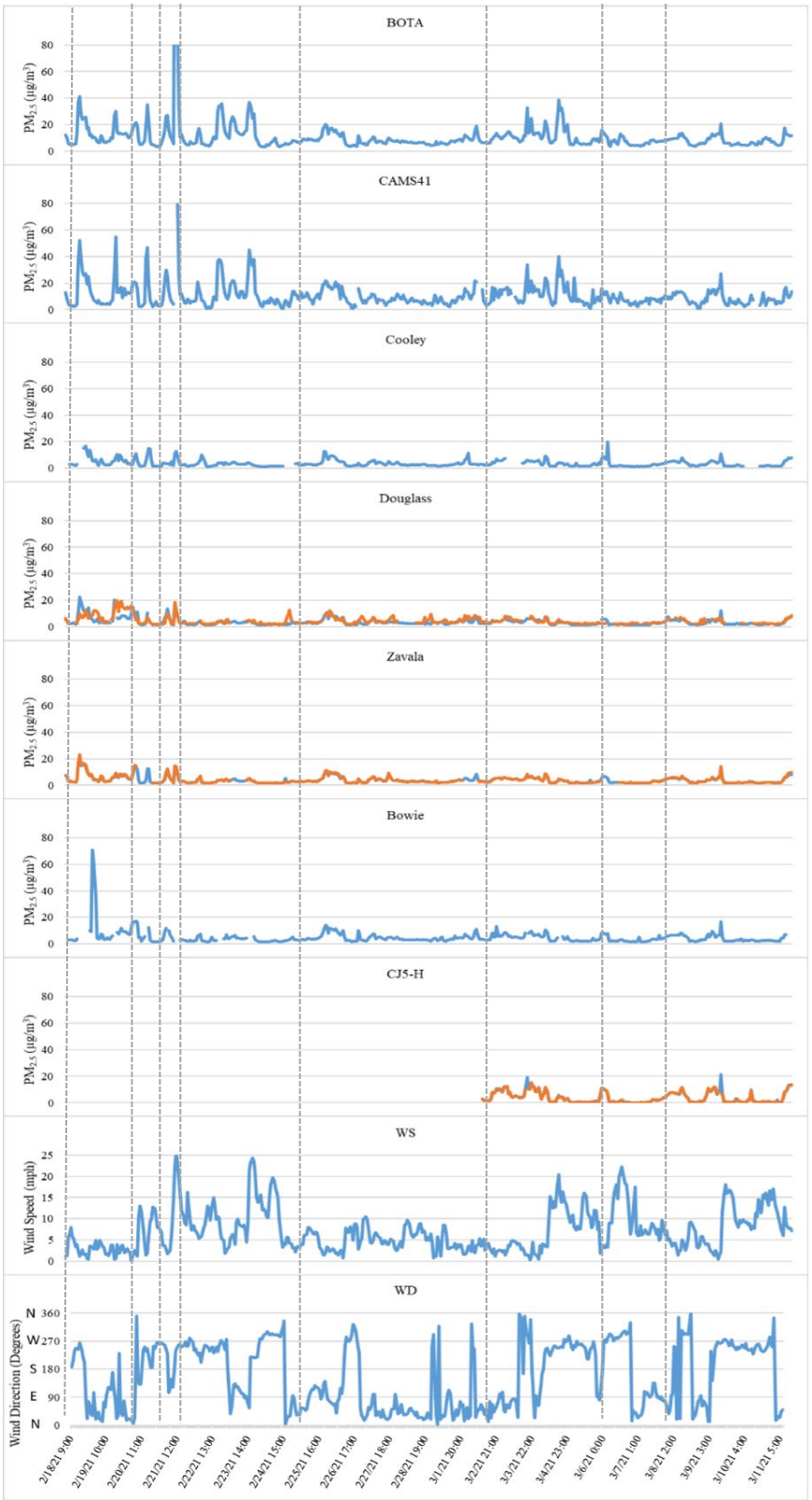

Figure 13. Community Purple Air $PM_{2.5}$ time series data and concurrent wind data. (Data collected from collocated monitors are colored in orange.)

Comparison of BOTA and TCEQ Measurements

TRAP concentrations are compared with the concurrently collected data at the CAMS 41 station located within 0.4 km from the BOTA in Figure 14. The hourly $PM_{2.5}$ and O_3 concentrations are well correlated between the BOTA and CAMS sites, with an R^2 value greater than 0.87 for each pollutant, while the correlation for NO_2 is moderate at 0.50. As is well reported in the literature, variation in near-road NO_2 concentrations is strongly affected by vehicle emissions, the complicated photochemical reactions near vehicle exhausts, local industrial sources, and local meteorological variability. Nevertheless, the agreement in the magnitude of NO_2 concentration between data collected in the heavy traffic at the BOTA and a central community monitoring site is worth noting. To further understand the level of TRAP pollution at the BOTA relative to other community locations, Table 8 lists available FRM TRAP concentrations reported in the PdN. $PM_{2.5}$ concentrations at the BOTA are comparable to those measured at CAMS 41 (an increase of ~2 percent in mean and ~1 percent in median) and slightly higher (an increase of ~25 percent in mean and ~10 percent in median) than a site 18 km away from the BOTA, suggesting that high background $PM_{2.5}$ concentrations exist in the PdN and that the BOTA PM emissions impose insignificant impact on the local PM air quality. O_3 concentration at the BOTA was lower than those observed at other PdN locations. It decreased by 8–50 percent in mean or by 12–58 percent in median as the location was further removed from the BOTA. The decrease of O_3 at the BOTA is the result of the combined effects of complex NO_2-O_3 photolysis and chemical reactions near the vehicle exhausts, solar radiation, and vehicle emissions. It strongly suggests that O_3 is likely ubiquitous in the PdN and the BOTA emissions do not significantly contribute to the local O_3 pollution. The in-traffic NO_2 measurements at the BOTA are strongly affected by the constant vehicle emissions surrounding the monitor and complicated by photochemical reactions and NO-NO_2 conversions. In this case with the BOTA station, one would expect it to have a higher concentration than that of the CAMS 41 station, which is in a less traveled area. This is supported in Table 8, which shows the period average for both sites where NO_2 concentration is higher at the BOTA than CAMS 41 by about 20 percent. Nevertheless, the levels of in-traffic NO_2 concentration at the BOTA, as well as in the community, are all well below the level of any health concern. This is supported in Table 9, which shows the period average for both sites. At the BOTA each station average is greater than 23 ppb, while at CAMS 41 it is only 18.7, a 20 percent decrease.

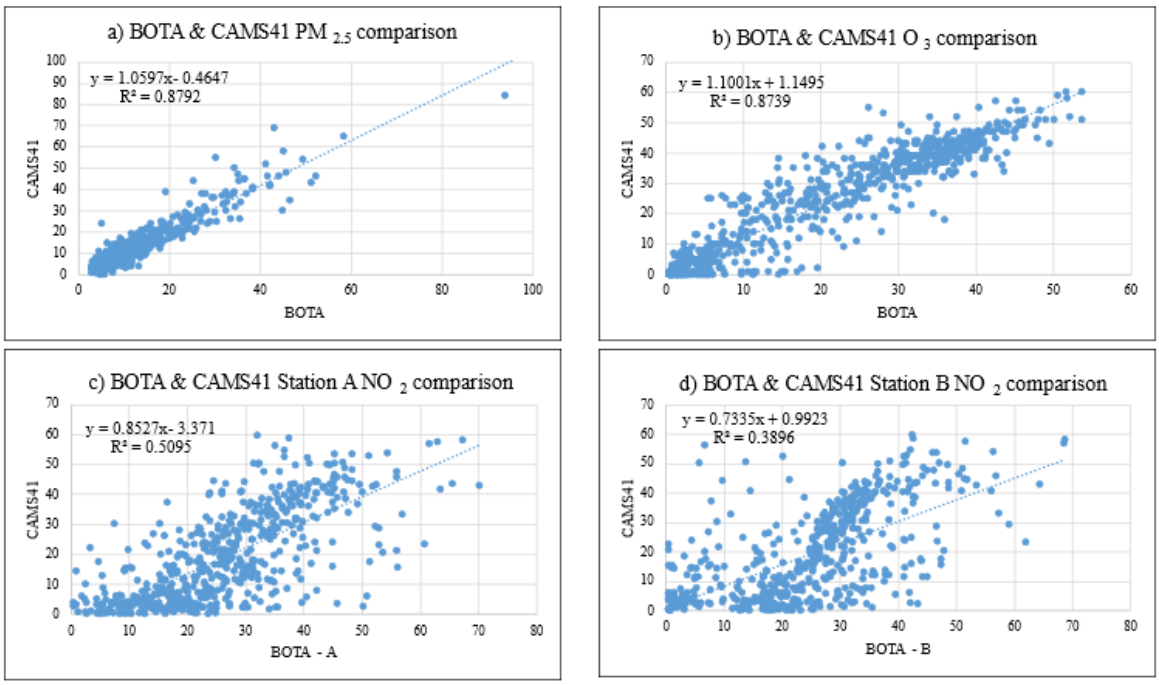

Figure 14. Pearson correlations between BOTA and CAMS 41 data: (a) $PM_{2.5}$, (b) O_3, (c) Station A NO_2, and (d) Station B NO_2.

Table 8. Period Summary Statistics for Regional Monitoring Stations in Comparison with BOTA Data.

Period Arithmetic Mean Value								
Measurement		BOTA	CAMS41	CAMS37	CAMS49	CAMS72	CAMS1011	CAMS1021
$PM_{2.5}$ (µg/m^3)		**11.6**	11.4	—	9.2	—	—	—
O_3 (ppb)		**22.2**	25.5	24.1	24.9	32.7	—	33.4
NO_2 (ppb)	A	**24.0**	18.7	15.5	—	—	15.1	—
	B	**23.1**						
Distance from BOTA (km)		—	0.4	5.1	18.2	14.3	4.2	14.0
Period Median Value								
Measurement		BOTA	CAMS41	CAMS37	CAMS49	CAMS72	CAMS1011	CAMS1021
$PM_{2.5}$ (µg/m^3)		**8.1**	8.0	—	7.4	—	—	—
O_3 (ppb)		**24.0**	29.5	28.0	27.0	37.0	—	38.0
NO_2 (ppb)	A	**23.3**	15.3	11.6	—	—	10.2	—
	B	**23.7**						
Distance from BOTA (km)		—	0.4	5.1	18.2	14.3	4.2	14.0

Table 9. Period Summary Statistics.

		Period Average			Period Median		
Pollutant		BOTA	CAMS41	Percent Difference	BOTA	CAMS41	Percent Difference
$PM_{2.5}$ (µg/m^3)		11.6	11.4	1.9	8.1	8.0	1.5
O_3 (ppb)		22.2	25.5	−14.8	24.0	29.5	−22.8
NO_2 (ppb)	A	24.0	18.7	22.2	23.3	15.3	34.2
	B	23.1		19.1	23.7		35.4

Table 10. Daylight Hours (6 a.m.–6 p.m.).

		Period Average			Period Median		
Pollutant		BOTA	CAMS41	Percent Difference	BOTA	CAMS41	Percent Difference
$PM_{2.5}$ (µg/m^3)		11.3	9.8	13.3	7.7	7.0	9.0
O_3 (ppb)		27.3	31.6	−16.0	30.4	36.0	−18.4
NO_2 (ppb)	A	21.8	14.4	34.0	20.8	11.1	46.9
	B	18.4		21.9	17.7		37.7

Table 11. Night Hours (7 p.m.–5 a.m.).

		Period Average			Period Median		
Pollutant		BOTA	CAMS41	Percent Difference	BOTA	CAMS41	Percent Difference
$PM_{2.5}$ (µg/m^3)		11.9	12.8	−7.3	8.8	9.0	−2.5
O_3 (ppb)		17.4	20.5	−17.9	15.8	22.0	−39.6
NO_2 (ppb)	A	28.0	22.4	20.0	27.3	21.3	22.0
	B	29.8		24.8	29.1		26.8

Figure 15 shows the concentrations of various pollutants at the BOTA and at CAMS 41. $PM_{2.5}$ concentrations at the BOTA follow almost exactly the trend of concentrations at CAMS 41. This is also true for O_3 concentrations. NO_2 concentrations at the BOTA show higher concentrations than at CAMS 41 but in general correlate well with the peaks and valleys in the data. Figure 16 shows the concentration polar plot of concentrations at the BOTA and at CAMS 41 relative to wind speed and wind direction measured at CAMS 41. Concentrations at both locations were higher when wind directions were coming from the southwest. This may imply that concentrations are increased when the wind direction causes the monitors to be downwind of border emissions.

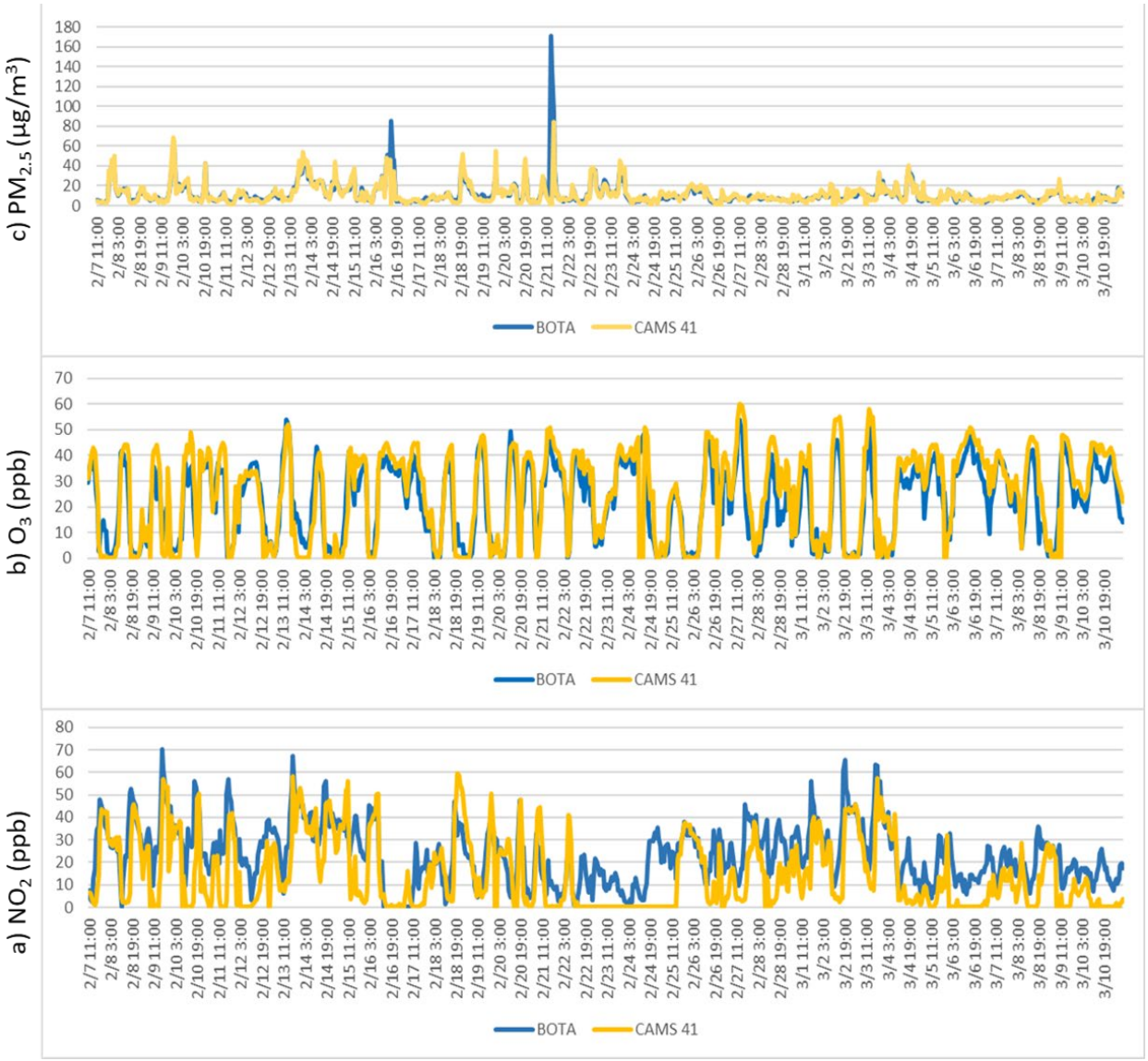

Figure 15. Time series of (a) $PM_{2.5}$, (b) O_3, and (c) NO_2 concentrations at BOTA and CAMS 41.

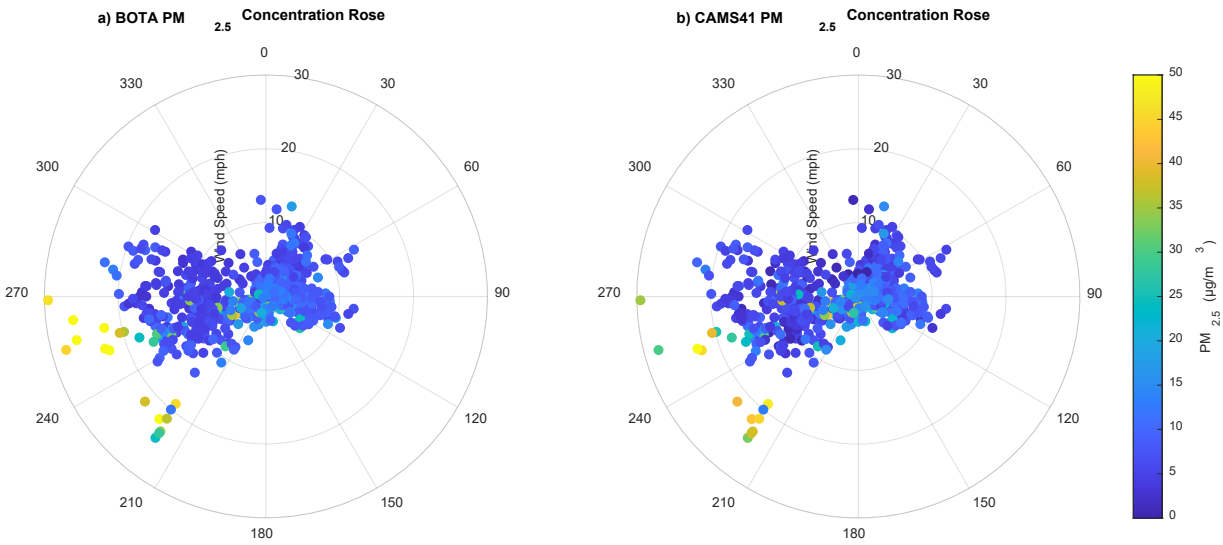

Figure 16. $PM_{2.5}$ concentration roses at BOTA and CAMS 41 sites.

TRAP Concentration on the BOTA

Table 8 shows that all three TRAP concentrations on the BOTA amidst the traffic queue are comparable to those observed in the community, implying that in-traffic TRAP concentrations may not be much different than those concentrations observed at CAMS 41. Our current observation of a 33-day averaged in-traffic $PM_{2.5}$ concentration of 11.6 µg/m^3 is remarkably close to the 8-week (2 weeks per season) $PM_{2.5}$ average of 11.3 µg/m^3, observed more than a decade ago at a near-road location (Figure 4) that is approximately 100 m south of the inspection booth (Olvera et al., 2013). One notices that both these two short-term $PM_{2.5}$ averages are below the annual NAAQS for $PM_{2.5}$ of 12 µg/m^3. In-traffic TRAP concentrations were recently reported for an urban road with a medium traffic volume of ~400–800 vehicles/hr and an average speed of 40 km/hr in Australia (Smit et al., 2019). Their on-road air samples were collected immediately adjacent to the road (i.e., within 1 m from road markings and the curb) in the study. On-road $PM_{2.5}$, PM_{10}, NO_2, and O_3 concentrations observed during this short-term study (9 hours during the day for two days) were low and well below the World Health Organization guideline concentrations and the NAAQS of the United States. The relatively small increases in on-road $PM_{2.5}$, PM_{10}, and O_3 concentrations from their respective urban backgrounds imply the prevalence of urban background PM and O_3 concentrations and that on-road TRAP concentrations are less affected by the variability in local vehicle emissions, traffic, and meteorological conditions. Furthermore, the study suggests that on-road NO_2 and O_3 concentrations are primarily driven by atmospheric chemistry processes and not significantly affected by variations in local traffic volume and fleet mix (Smit et al., 2019). In another relevant study, TRAP concentrations on the pedestrian pathway that is approximately 5 m from the vehicle inspection lane at the San Ysidro POE were collected by Galaviz et al (Galaviz et al., 2014). The mean $PM_{2.5}$ concentration observed at this fixed location was found to be only about 14 percent higher than the personal exposure concentration observed in the San Ysidro community, which is about 0.4 km away from this POE pedestrian pathway. If the averaged community exposure at San Ysidro was to be represented by the personal exposure concentration in the community (Quintana et al., 2014), then the near in-traffic $PM_{2.5}$ concentration at the busy San Ysidro POE displayed a level only slightly elevated from the exposure concentration observed in the community.

Comparison of BOTA and Near-Road Community Measurements

Data Correction

Purple Air sensors were calibrated in late January and early February 2022. The low-cost sensors report $PM_{2.5}$, temperature, and humidity; these parameters were first used to verify each sensor's validity. The performance and accuracy of the Purple Air sensors in various locations across the United States have been extensively reviewed and reported (Ardon-Dryer et al., 2020; Barkjohn et al., 2021; Kelly et al., 2017; Tryner et al., 2020). Although the Purple Air sensor correlated well

with FRM/FEM instruments in ambient conditions, its response varies with particles and may exhibit a non-linear response when $PM_{2.5}$ concentrations are high (Kelly et al., 2021). Several studies have found that the instruments were affected by humidity, although many studies also have reported a negligible effect of temperature and relative humidity on Purple Air's performance (Ardon-Dryer et al., 2020; Magi et al., 2020).

We first applied a multiple linear regression (MLR) analysis at CAMS 49 between the collocated Purple Air and FRM $PM_{2.5}$ data and developed the following regression equation:

$$C_{FRM} = \beta 0 + \beta 1 \bullet C_{obs} + \beta 2 \bullet HR + \beta 3 \bullet Temp + \mathcal{E} \qquad (2)$$

where C_{FRM}: FRM $PM_{2.5}$ concentration;
C_{obs}: the observed Purple Air $PM_{2.5}$ concentration;
$\beta 0$: the intercept;
$\beta 1$: fraction coefficient for C_{obs};
$\beta 2$: fraction coefficient for humidity effect;
$\beta 3$: fraction coefficient for temperature effect;
$\mathcal{E}$: error;
Temp: ambient temperature reported by Purple Air (^{o}C); and
HR*:* relative humidity reported by Purple Air (percent).

Table 12 lists the values for the regression parameters and the coefficients of determination. The impact of temperature and humidity on Purple Air's performance is not negligible and in an inconsistent negative direction. This unique behavior of Purple Air may be caused by the arid weather with low humidity, wide temperature fluctuation during the day, high altitude, and geologic source-dominated $PM_{2.5}$ (i.e., a higher percentage of larger geologic PM in $PM_{2.5}$) in our region. Ardon-Dryer et al. (2020) observed similar effects in Denver, Colorado, a city with similar atmospheric conditions and high altitude, although the impact is not as pronounced as in our study. Because of the negative impact of temperature and humidity on Purple Air's performance, we performed a simple linear regression (SLR) analysis, $C_{FRM} = A \bullet C_{obs} + B$, and the results are also shown in Table 12. Purple Air sensors could overestimate $PM_{2.5}$ from a few percent to nearly 100 percent. Nevertheless, the simple linear regression neglecting the temperature and humidity effect performed satisfactorily with comparable R^2 values.

Figure 17 shows one example of the corrected data for one of the Purple Air sensors using MLR and SLR analysis in comparison to the reference data at CAMS 49. The time series plots in the figure show that the multilinear adjustment catches the high concentrations (> 10 $\mu g/m^3$) better than the SLR analysis, whereas the SLR analysis performs better in low concentrations (between 0 and 10 $\mu g/m^3$). While the R^2 value for the data corrected using MLR is higher than for the data corrected using SLR (0.738 versus 0.672), the data becomes overly smoothed compared to the reference data (CAMS). This is because SLR adjustment tends to suppress the high concentrations, whereas MLR tends to raise the low concentrations for a better linear fit. The MLR adjustment has a propensity to overestimate concentrations more frequently than the SLR adjustment since low concentrations (< 10 $\mu g/m^3$) occurred more frequently during this study period. In addition, the adjusted mean and median values based on MLR were only slightly higher than the SLR adjusted data. For the above reasons, the SLR was used to adjust all $PM_{2.5}$ data in our study. The low-cost Purple Air sensors used throughout the study were equipped with dual Plantower PMS50003 sensors, named channel A and channel B. These channels generate a two-minute average for each of the sensors. These channel comparisons are used as an indicator of sensor malfunctioning. All sensors showed excellent linearity between channels A and B in our study. Most of the sensors maintained an R^2 value of 0.9 and above between channels, except one sensor. Table 12 shows in the last two columns that the sensor performed reasonably well and consistently between the collocated sensors used for duplicate sampling before and during the field study.

Table 12. Purple Air Correction Regression Analysis.

Sensor	Multiple Linear Regression					Simple Linear Regression			Sensor Performance	
	β0	β1	β2	β3	R^2	A	B	R^2	Inter-channel Performance (R^2)	Inter-device Performance (R^2)
Cooley	7.45	0.54	−0.18	−0.15	0.85	0.47	1.33	0.67	0.98	NA
Douglass 1	6.74	0.57	−0.18	−0.13	0.84	0.47	1.34	0.66	0.98	0.51
Douglass 2	7.39	0.64	−0.18	−0.11	0.86	0.51	1.52	0.66	0.99	
Zavala 1	6.63	0.64	−0.16	−0.1	0.84	0.56	1.69	0.67	0.96	0.99
Zavala 2	5.1	0.64	−0.1	−0.07	0.86	0.58	1.66	0.66	0.82	
Bowie	5.93	0.52	−0.19	−0.02	0.62	0.62	1.65	0.23	0.99	NA
CJ5-H 1	8.44	0.69	−0.20	−0.16	0.86	0.49	1.45	0.68	0.98	0.99
CJ5-H 2	5.49	0.58	−0.15	−0.06	0.85	0.54	2.82	0.22	0.95	

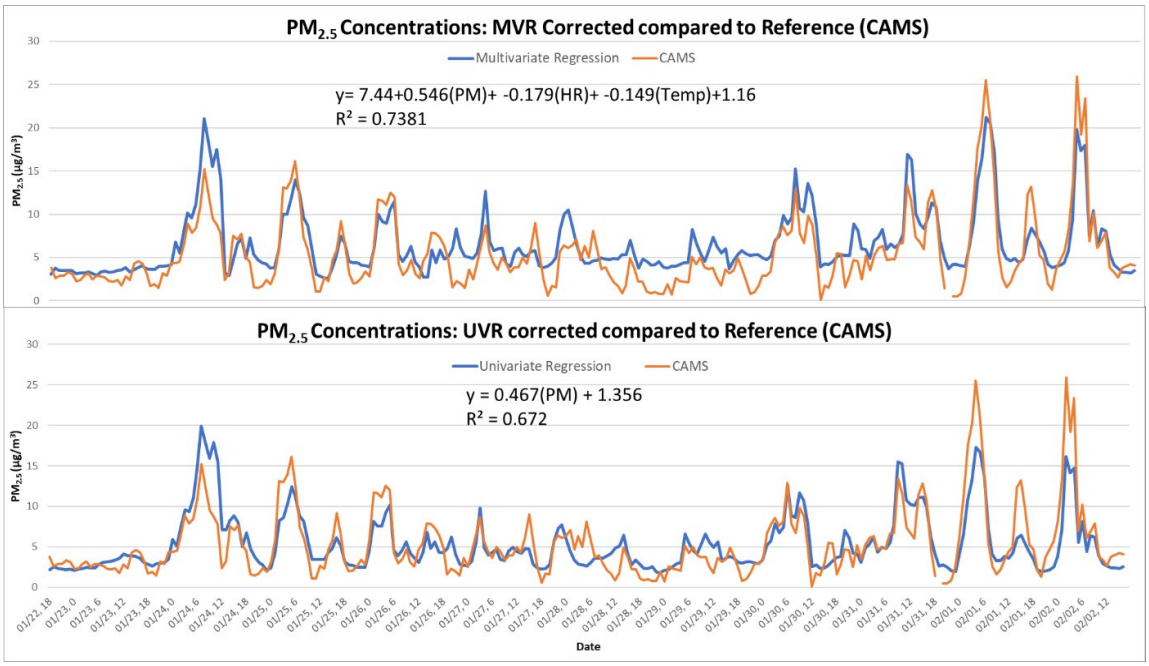

Figure 17. MLR corrected data and SLR corrected data compared to reference data.

$PM_{2.5}$ in the Community

In general, $PM_{2.5}$ concentrations observed in the residential community were lower than those measured at the BOTA and CAMS 41 stations. The mean and median values for each of the community sites are shown in box plots in Figure 18 .

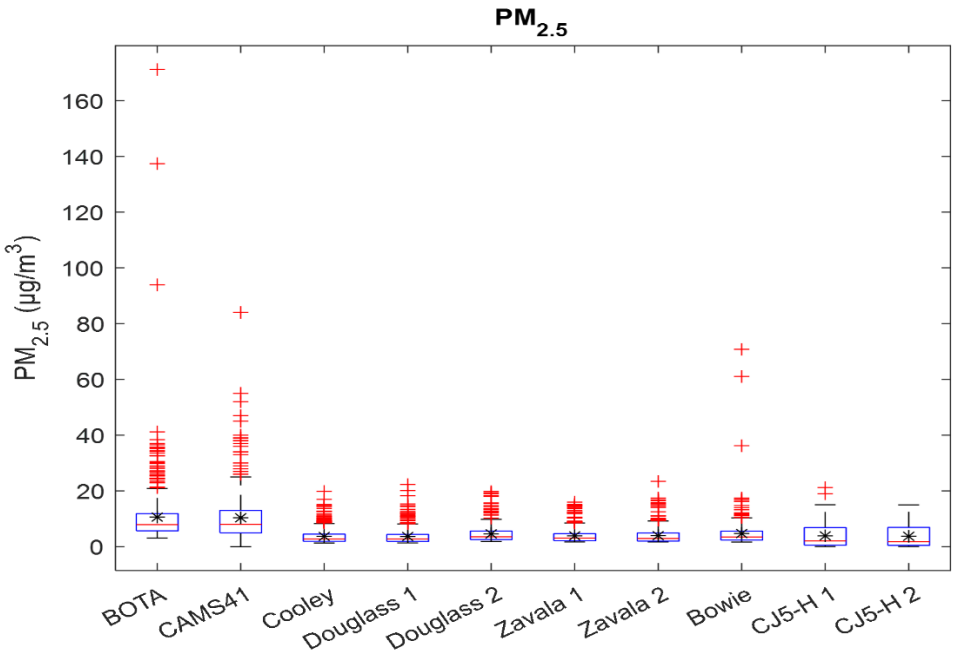

Figure 18. $PM_{2.5}$ box plots for community Purple Air $PM_{2.5}$ data.

These values are lower than the data recorded at the BOTA or CAMS 41, but similar among all sites with concentrations approximately 40–50 percent lower than the results reported from FRM instruments at CAMS 41 and 49. The low $PM_{2.5}$ concentrations in the community deserve further study in the future, and the performance of the Purple Air sensors in the arid region warrants additional investigation.

Concentration Estimates Predicted by AERMOD Modeling

Impacts of Queue Length on Exposure Concentrations

AERMOD was first used to evaluate the impacts of vehicle queue length on POE users due to prolonged wait time. By conducting a queue length analysis by varying the sources modeled, we can estimate the on-site and off-site concentrations at different queue lengths caused by various wait times on the BOTA. The queue length analysis was performed using a base emission rate at the volume sources and by including several scenarios with varying queue length. The results of the concentration estimates per unit emission rate at different queue lengths are shown in Figure 19. The impact of concentrations from the BOTA emissions stabilize as the total source area increases, particularly for on-site concentrations (Station A and B). Figure 19 also shows an isolated view of the results for the off-site locations. The closest site, the Chamizal site, can be seen to be more greatly affected (higher slope) than the other off-site concentrations. These results suggest that even with longer queues past 100 m, the in-traffic concentrations at the POE would stabilize at a "maximum" level. On the contrary, the concentration estimates at a distance away from the source are more sensitive to the size of the source (the queue length or the wait time of the POE traffic).

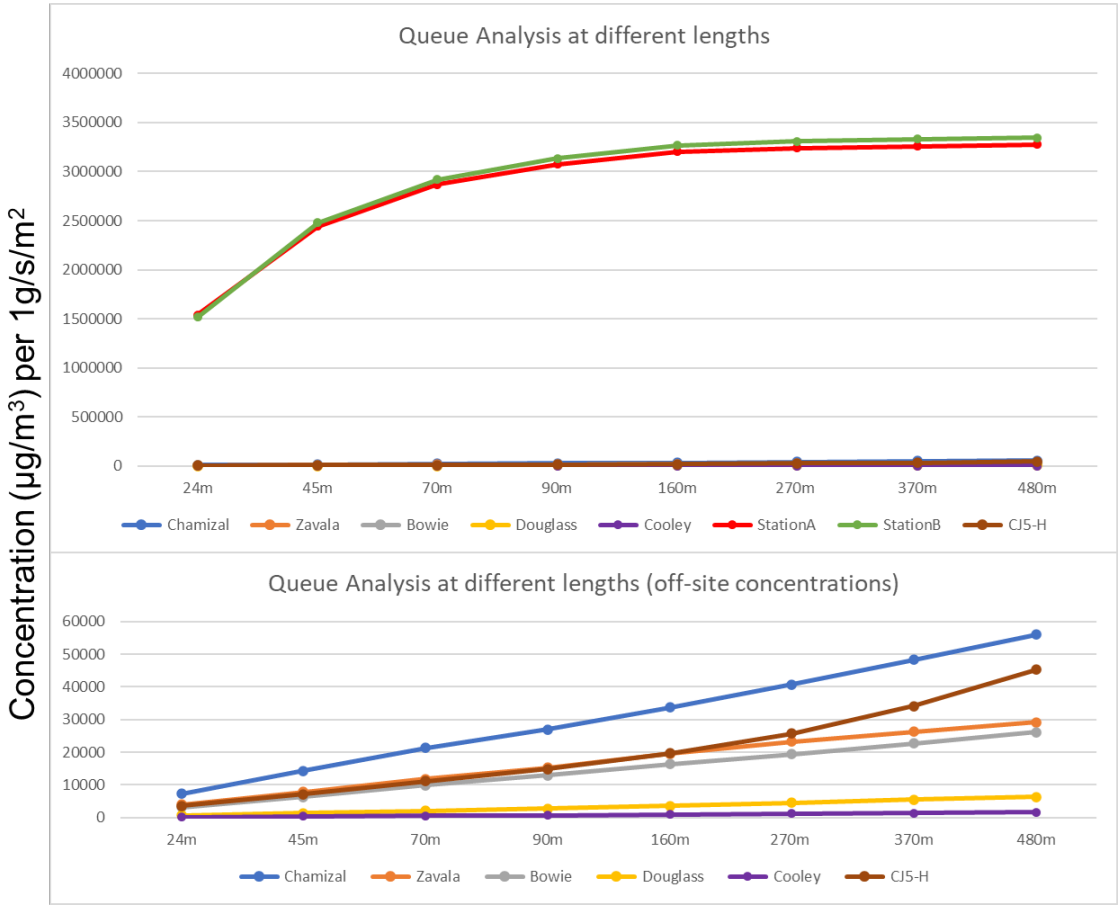

Figure 19. Queue analysis of modeled results at monitoring sites.

Cross-Roadway Concentration Distribution

The dispersion of concentrations from the roadway were also analyzed with the placement of receptors at increasing distances from the roadway, specifically in the direction perpendicular to the roadway. Figure 20**Error! Reference source not found.** shows the location of these receptors relative to the BOTA POE lanes and roadway.

Figure 20. Cross-roadway receptor placement.

A general rapidly decreasing trend of the modeled $PM_{2.5}$ concentrations with increasing distance from the center of the roadway and lanes was observed. Figure 21**Error! Reference source not found.** shows the dispersion of the pollutant $PM_{2.5}$ away from the roadway, where the concentration of airborne particles was characterized as a function of distance from the BOTA POE, with negative values representing the distance increasing to the west of the roadway. These results suggest

that the vast majority of dispersion occurs within 200 m of the highway. $PM_{2.5}$ concentrations decrease by tenfold within 100 m from the center of the BOTA. These results can be useful to urban planners and engineers and provide guidance on the safe placement of pedestrian walkways, border patrol agent offices, and other business activities to reduce human exposure to these concentrations.

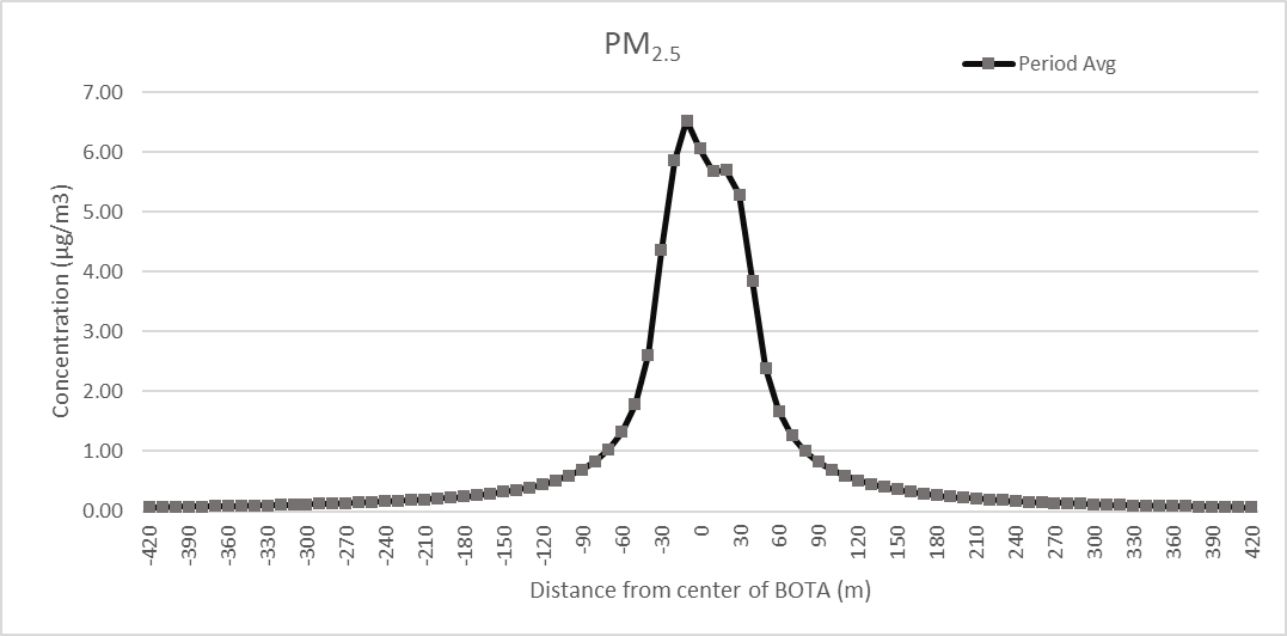

Figure 21. Modeled $PM_{2.5}$ dispersion as a function of distance from the highway.

Comparison of Modeled and Monitored Concentrations Using Calculated Seasonal Emission Rates

AERMOD analysis provided hourly modeled predictions for each pollutant during the study period at various discrete receptors representative of monitoring sites and key locations in the study area. These results were then compared to the hourly monitored concentrations obtained from in-field air monitoring sensors during the study period, in particular, the two monitors located inside the POE traffic (Monitor A and Monitor B). Only the results for the maximum queue length at the BOTA are presented in this section of discussion. Figure 22 shows the hourly modeled results for each pollutant compared to the actual monitoring results for the study period for the monitors located inside the POE. Hourly concentrations from the reference site (CAMS 41) for $PM_{2.5}$ and NO_2 are also shown in Figure 22. The 792 hours of the study period were processed, with 109 calm hours according to low wind speeds in the meteorological data file. These calm hours cannot produce a concentration estimate due to the Gaussian model employed by AERMOD, and this accounts for around 14 percent missing hours during the study period.

$PM_{2.5}$ modeled results trend closely to the monitored $PM_{2.5}$ data, with peaks and valleys in concentration levels following similar patterns. Considering that AERMOD analysis employs many standardized factors such as the ERs, it is interesting to see how closely hourly predicted concentrations trend with monitored concentrations with rising peaks and sinking valleys in Figure 22a. PM_{10} modeled results on average are similar to the monitored PM_{10} data, but maximum monitored hourly values are much higher, which is expected considering that PM_{10} in this geological area is largely driven by desert dust. NO_2 modeled results were seen to deviate from the monitored results. This may be due to the greater instability of NO_2 production in the atmosphere, which depends on the photovoltaic reaction between NOx compounds and atmospheric O_3 molecules. Nevertheless, meteorology and emission characteristics were well captured in the AERMOD analysis, where both modeled and monitored results trend in similar fashions, as seen in Figure 22b and Figure 22c.

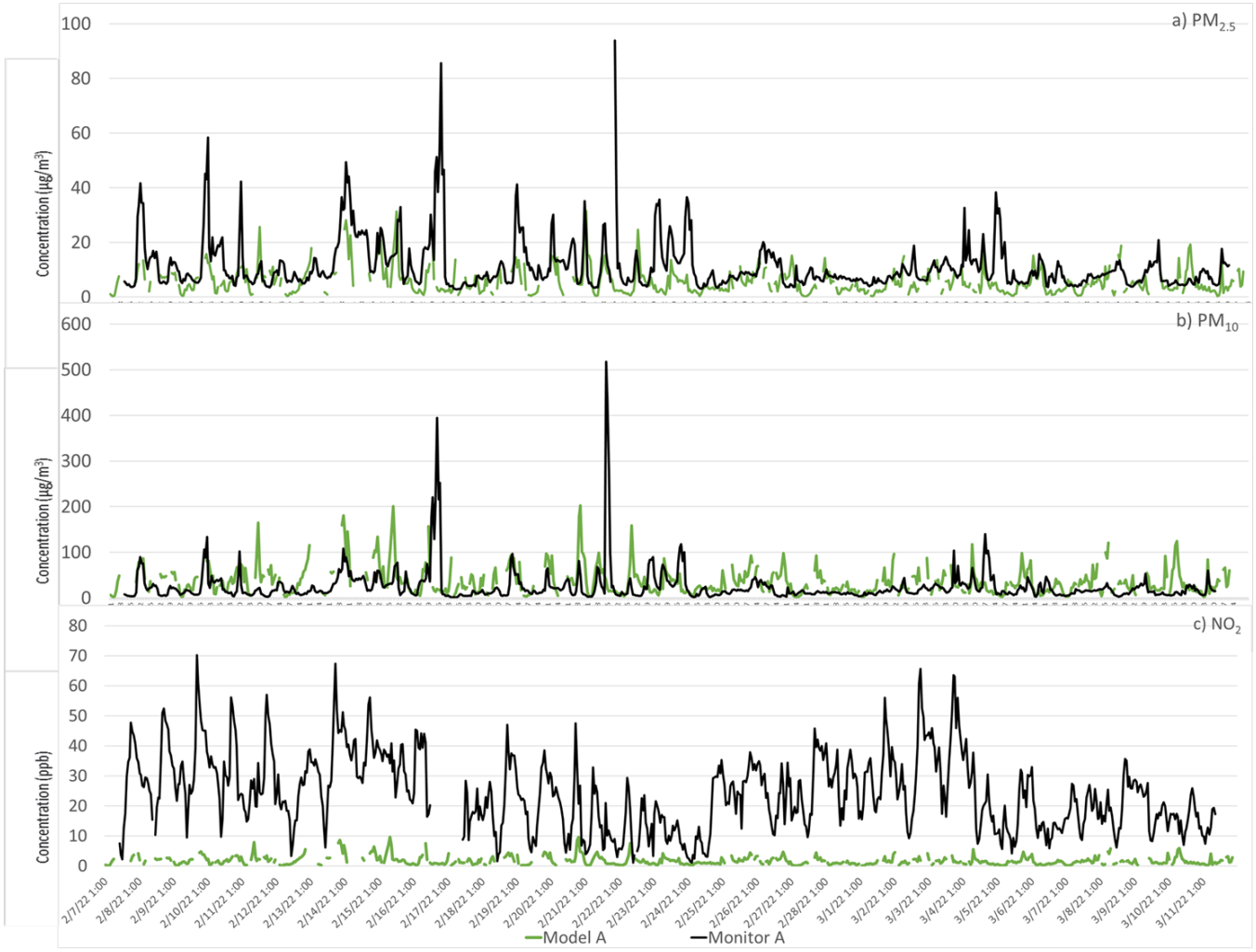

Figure 22. Hourly modeled and monitored results: (a) $PM_{2.5}$, (b) PM_{10}, and (c) NO_2.

The 24-hr averages for the study period for the modeled and monitored values of pollutant concentrations are shown in Figure 23. This averaging level can better illustrate the connection between the modeled concentrations and the monitored concentrations observed in the POE. Modeled $PM_{2.5}$ averages trend well with the actual monitored values but occur at lower concentrations. As reported in the literature, background $PM_{2.5}$ concentrations constitute approximately 85 percent of the near-road $PM_{2.5}$ concentrations. In other words, vehicle emissions contribute to approximately 15 percent of the near-road $PM_{2.5}$ concentrations. It is thus expected that vehicle emissions will contribute more than 15 percent of the $PM_{2.5}$ observed on road or in traffic and that the background $PM_{2.5}$ concentrations would still be a major contributor to the on-road $PM_{2.5}$ concentrations. Modeled PM_{10} averages also trend well with monitored averages but are consistently higher than the monitored 24-hr averages with a few exceptions. Higher modeled PM_{10} concentration estimates are likely the results of higher PM_{10} emission estimates. The few exceptions with higher estimated PM_{10} are due to occasional dust events in the region. Desert dust makes up the majority of PM_{10} in this region, so it is not surprising to see the occasional deviation of estimated PM_{10} from the monitored PM_{10}. Modeled 24-hr-averaged NO_2 is quite low compared to the monitored 24-hr averages. Although the in-traffic modeled and monitored NO_2 concentrations are expected to be closely correlated on road, atmospheric levels of NO_2 may be overly influenced by variables like sunlight and other volatile organic compounds (VOC) concentrations. The comparison of the in-traffic modeled to monitored results indicates that atmospheric levels of NO_2 near emission sources may be significantly influenced by the complex NO_2-O_3 photolysis and interactions of NOx with variables like sunlight and other VOC concentrations.

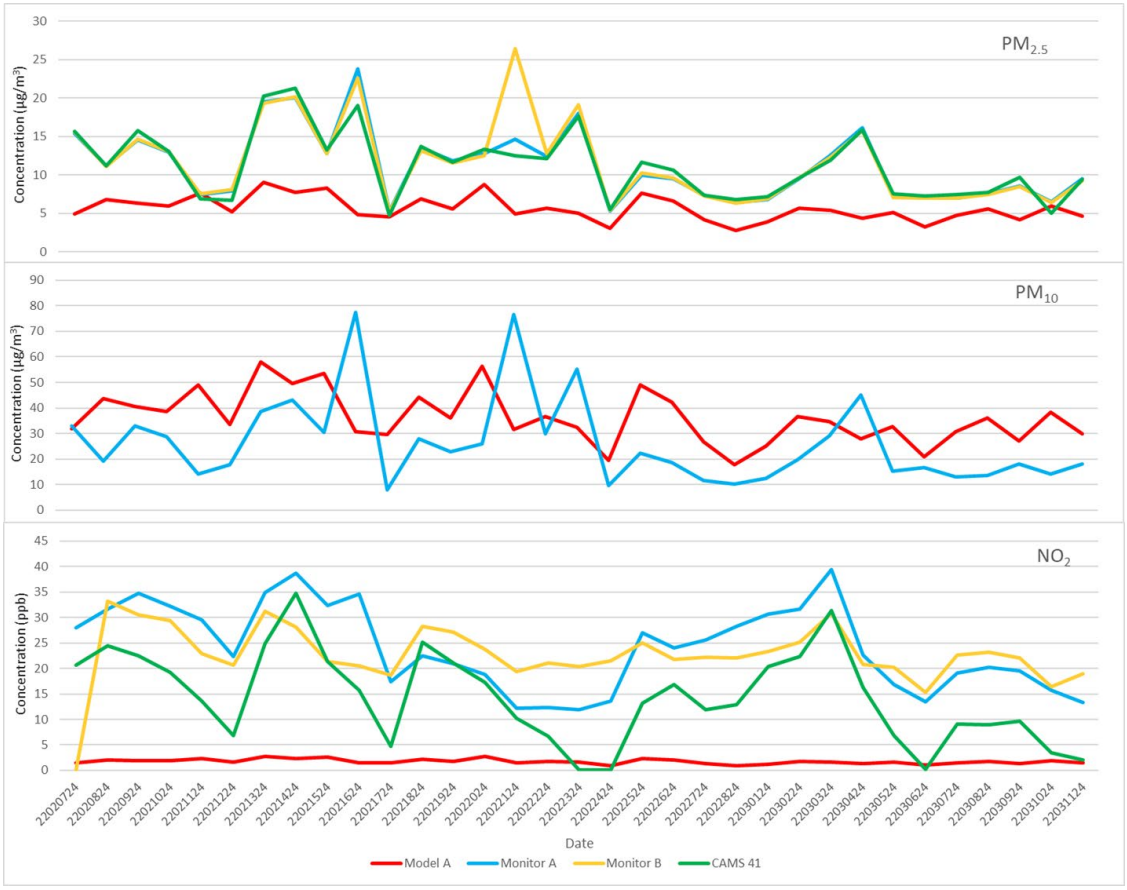

Figure 23. 24-hr averages of modeled and monitored data.

Descriptive statistics of modeled and monitored data are shown in Table 13. For $PM_{2.5}$, the period average of the modeled results is 51 percent of monitored levels of $PM_{2.5}$. In addition, the 1-hr max and 24-hr max of modeled data account for around 33 percent and 38 percent of monitored $PM_{2.5}$, respectively. For PM_{10}, the period average of model results is higher than the monitored average (136–147 percent), but the 1-hr max from modeled results is only around 40 percent of the monitored PM_{10} and the 24-hr max is around 70 percent of the monitored 24-hr max PM_{10}. As mentioned before, occasional dust events during the study period are the cause for the sudden increases in the monitored results. The modeled NO_2 results are generally lower than the monitored NO_2 levels at a level of approximately 14 percent, 29 percent, and 15 percent of the monitored data for period average, 1-hr max, and 24-hr max, respectively.

Assessment of Community Exposure Resulting from the BOTA Emissions

For the community sites, where monitoring was conducted at 10 school locations using the low-cost Purple Air sensors, the period average of the modeled $PM_{2.5}$ accounted for around 1 percent of monitored $PM_{2.5}$ observed at each site indicating the minimal impacts of BOTA emissions on the community. However, when looking at the 1-hr max, Zavala and CJ5-H showed that modeled $PM_{2.5}$ concentrations account for 11 percent of monitored 1-hr max $PM_{2.5}$ concentrations. Additionally, Zavala and CJ5-H showed that modeled $PM_{2.5}$ concentrations account for around 5 percent of monitored 24-hr max $PM_{2.5}$ concentrations. The adverse atmospheric meteorological conditions such as low wind conditions and temperature inversions in the region are likely the cause for these concentration spikes. When comparing the NO_2 modeled period average, 1-hr max, and 24-hr max to

the respective values of monitored NO_2, modeled concentrations account for 7.2 percent, 14 percent, and 7 percent, respectively. Table 13, Table 14, and

Table 15 summarize the comparisons of modeled and monitored pollutant concentrations at the community locations for all period average, 1-hr max, and 24-hr max data.

Table 13. Descriptive Statistics of Modeled and Monitored Data (Period Average).

	Modeled			Monitored			Ratio (Model/Monitor)		
	$PM_{2.5}$ ($\mu g/m^3$)	PM_{10} ($\mu g/m^3$)	NO_2 (ppb)	$PM_{2.5}$ ($\mu g/m^3$)	PM_{10} ($\mu g/m^3$)	NO_2 (ppb)	$PM_{2.5}$ (percent)	PM_{10} (percent)	NO_2 (percent)
StationA	5.73	36.90	1.75	11.20	25.13	24.23	51	147	7.2
StationB	5.86	37.73	1.79	11.55	27.64	23.25	51	136	7.7
CAMS41	0.08	0.49	0.02	11.17	—	14.29	0.7	—	0.2
Bowie	0.03	0.21	0.01	4.72	—	—	0.7	—	—
Zavala	0.05	0.32	0.02	3.92	—	—	1	—	—
CJ5-H	0.08	0.51	0.02	3.81	—	—	2	—	—
Douglass	0.01	0.05	0.00	4.12	—	—	0.2	—	—
Cooley	0.00	0.01	0.00	3.68	—	—	0.1	—	—
TollBooth	3.80	24.44	1.16	—	—	—	—	—	—
Office	1.81	11.69	0.55	—	—	—	—	—	—
EastPedestrian	4.28	27.59	1.31	—	—	—	—	—	—
SBToll	1.72	11.07	0.52	—	—	—	—	—	—
WestPedestrian	1.26	8.13	0.39	—	—	—	—	—	—

Note: — = not available.

Table 14. Descriptive Statistics of Modeled and Monitored Data (1-hr Max).

	Modeled			Monitored			Ratio (Model/Monitor)		
	$PM_{2.5}$ ($\mu g/m^3$)	PM_{10} ($\mu g/m^3$)	NO_2 (ppb)	$PM_{2.5}$ ($\mu g/m^3$)	PM_{10} ($\mu g/m^3$)	NO_2 (ppb)	$PM_{2.5}$ (percent)	PM_{10} (percent)	NO_2 (percent)
StationA	31.39	202.16	9.59	93.92	517.28	70.23	33	39	14
StationB	37.34	240.47	11.41	167.48	580.23	68.67	22	41	17
CAMS41	2.25	14.52	0.69	84.00	—	59.60	3	—	1
Bowie	1.33	8.59	0.41	70.77	—	—	2	—	—
Zavala	2.14	13.81	0.65	19.70	—	—	11	—	—
CJ5-H	2.00	12.90	0.61	18.07	—	—	11	—	—
Douglass	0.47	3.03	0.14	21.02	—	—	2	—	—
Cooley	0.12	0.77	0.04	19.81	—	—	1	—	—
TollBooth	33.07	212.95	10.10	—	—	—	—	—	—
Office	28.49	183.48	8.70	—	—	—	—	—	—
EastPedestrian	37.22	239.70	11.37	—	—	—	—	—	—
SBToll	29.90	192.56	9.13	—	—	—	—	—	—
WestPedestrian	18.74	120.69	5.72	—	—	—	—	—	—

Note: — = not available.

Table 15. Descriptive Statistics of Modeled and Monitored data (24-hr Max).

	Modeled			Monitored			Ratio (Model/Monitor)		
	$PM_{2.5}$ ($\mu g/m^3$)	PM_{10} ($\mu g/m^3$)	NO_2 (ppb)	$PM_{2.5}$ ($\mu g/m^3$)	PM_{10} ($\mu g/m^3$)	NO_2 (ppb)	$PM_{2.5}$ (percent)	PM_{10} (percent)	NO_2 (percent)
StationA	9.00	57.99	2.75	23.79	85.10	39.37	38	68	7.0
StationB	9.30	59.91	2.84	26.42	82.15	33.27	35	73	8.5
CAMS41	0.30	1.91	0.09	21.25	—	34.70	1	—	0.3
Bowie	0.13	0.81	0.04	13.65	—	—	1	—	—
Zavala	0.30	1.95	0.09	8.52	—	—	4	—	—
CJ5-H	0.36	2.35	0.11	8.08	—	—	5	—	—
Douglass	0.05	0.31	0.01	8.24	—	—	1	—	—
Cooley	0.01	0.05	0.00	6.35	—	—	0.1	—	—
TollBooth	8.34	53.68	2.55	—	—	—	—	—	—
Office	7.30	47.00	2.23	—	—	—	—	—	—
EastPedestrian	9.63	62.01	2.94	—	—	—	—	—	—
SBToll	5.71	36.79	1.74	—	—	—	—	—	—
WestPedestrian	4.21	27.14	1.29	—	—	—	—	—	—

Note: — = not available.

The spatial distributions of $PM_{2.5}$ concentrations in the community at the maximum 1-hr, maximum 24-hr average, and all-period averages are shown in Figure 24. The figure provides a clearer illustration of the $PM_{2.5}$ exposure in the community due to the traffic emissions from the BOTA. All three time-averaged $PM_{2.5}$ concentrations decrease rapidly from the BOTA towards the residential community.

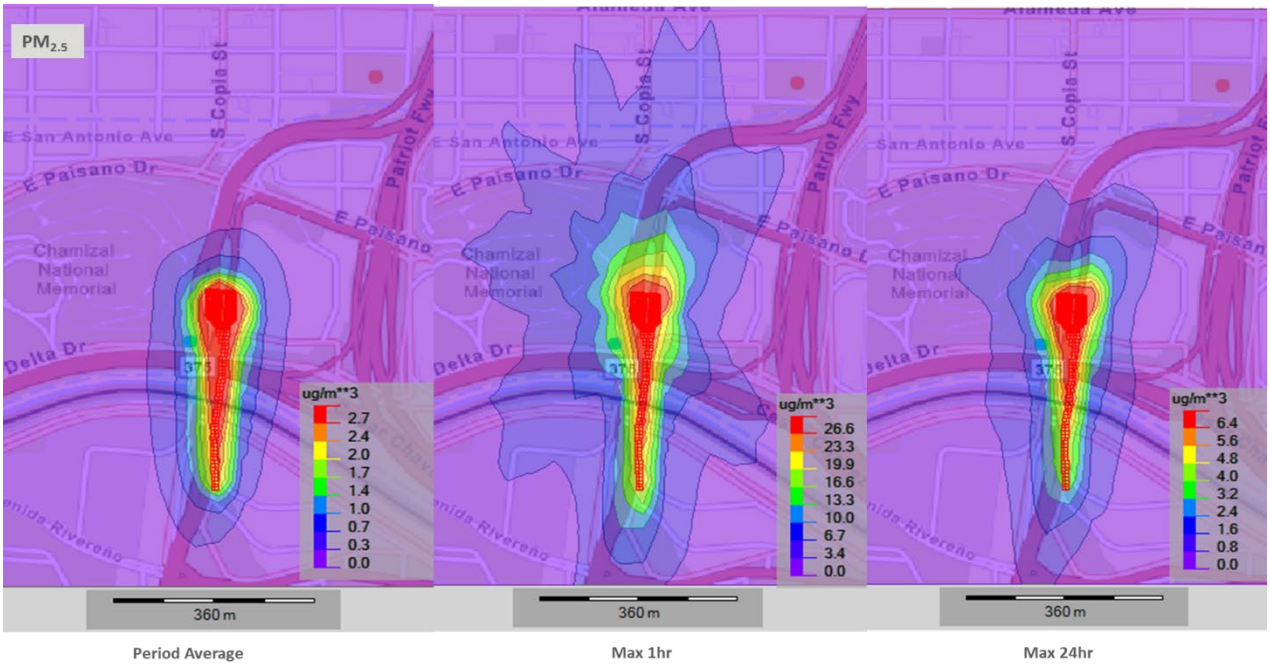

Figure 24. Period average, max 1-hr, and max 24-hr PM2.5 concentration estimates.

Similarly, Figure 25 and Figure 26 show the spatial distributions of PM_{10} and NO_2 concentrations in the community at the maximum 1-hr, maximum 24-hr average, and all-period averages, respectively. The spatial distributions of these pollutants closely resemble the distribution for $PM_{2.5}$ concentrations.

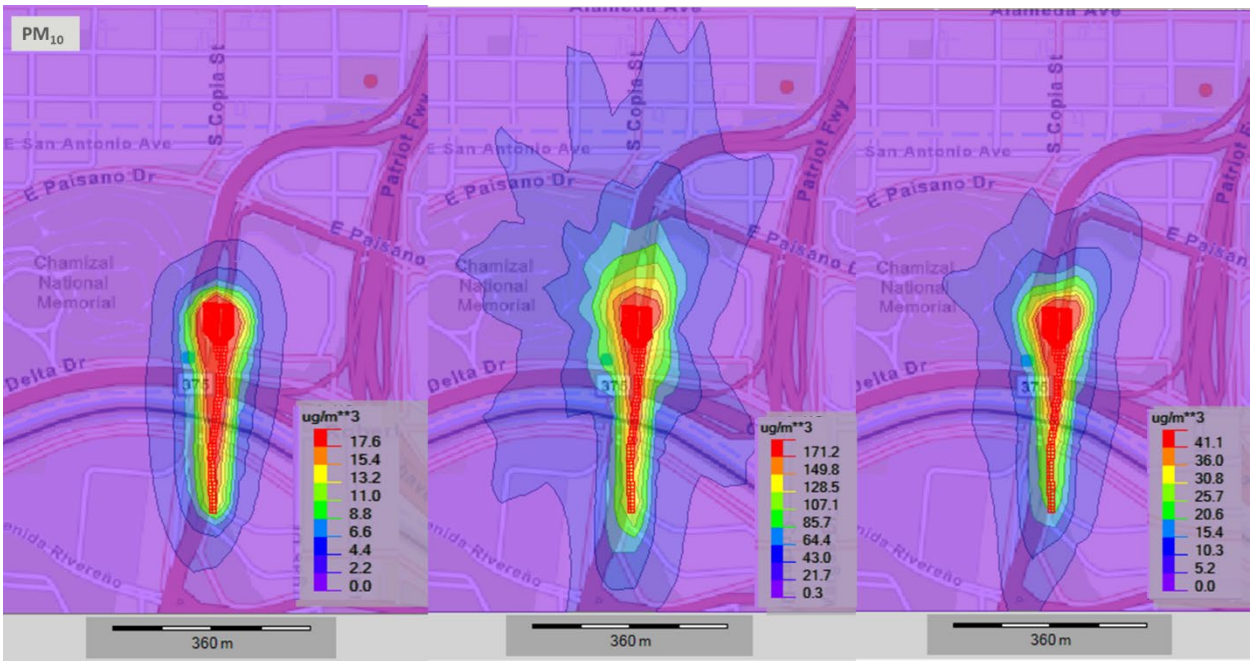

Figure 25. Period average, max 1-hr, and max 24-hr Pm_{10} concentration estimates.

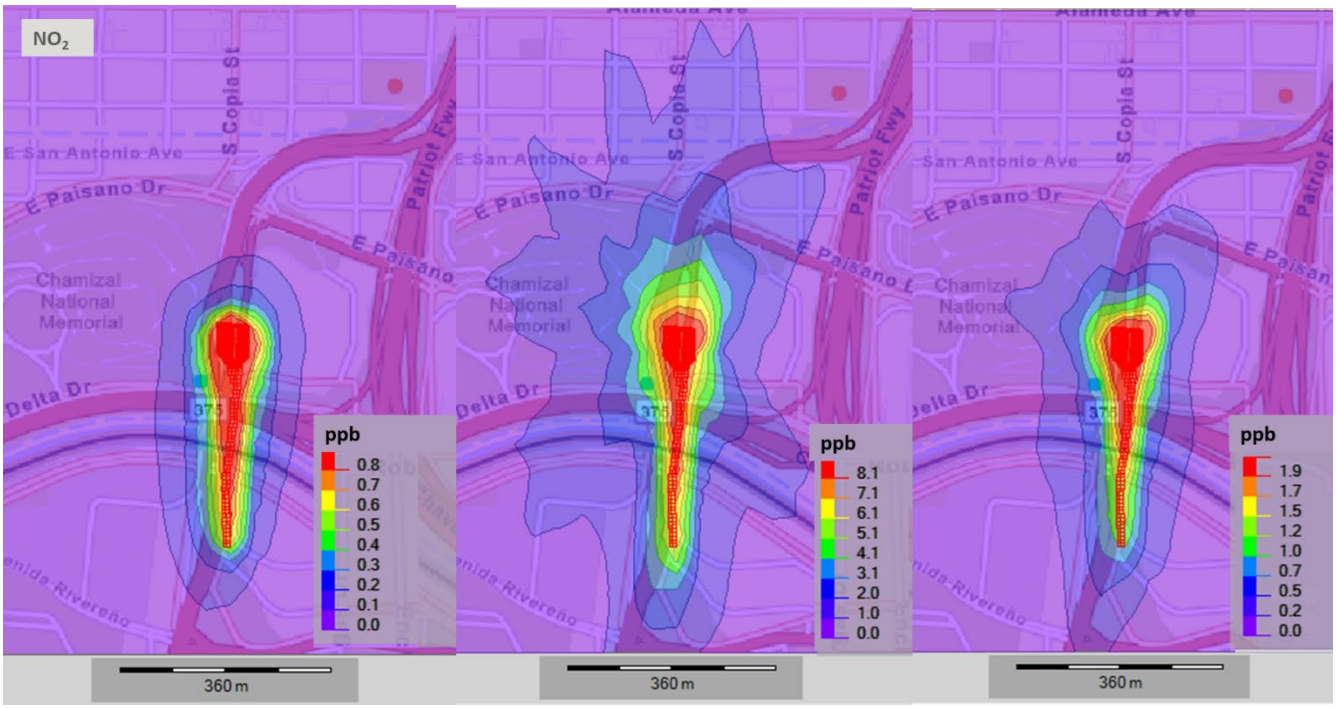

Figure 26. Period average, max 1-hr, and max 24-hr No_2 concentration estimates.

These concentration heat maps are able to spatially identify which areas and receptors near the BOTA experience the highest levels of impacts. Because the difference in modeling is based on the ERs, the distribution of the pollutant concentrations is the same but scaled to the different ERs for $PM_{2.5}$, PM_{10}, and NO_2. The exposure heat maps, which show the spatial distribution of the pollutant concentrations estimated by the model, indicate that the impact of the BOTA on receptors reaches around 200 m. However, at this maximum distance of 200 m, receptors are only exposed to about 10 percent of

impacts relative to the center of the BOTA. The spatial distribution maps also indicate the receptors north of the BOTA experience the highest levels of impact, especially for the estimated 1-hr max concentrations.

The discrete receptors listed in Table 13, Table 14, and

Table 15 are used to represent an overview of how the surrounding areas respond to the traffic-related emissions from the BOTA. The TollBooth modeled concentration value represents the average of multiple receptors along the width of the toll booth lanes to represent the pollutant exposure of the toll booth workers. The period-averaged model concentration estimate at the toll booth is around 30 percent less than the modeled concentration inside the BOTA at the location of Station A. However, the modeled 1-hr max at the toll booth is actually 5 percent higher than the modeled 1-hr max estimated inside the BOTA. This is likely due to the prevailing hourly wind direction being from southwest, positioning the toll booth downwind of the BOTA emissions. Another receptor of importance is the EastPedestrian receptor, which is placed at the end of the pedestrian walkway as border-crossing individuals walk and enter the U.S. Customs building. The period average for $PM_{2.5}$ at this receptor is 4.28 $\mu g/m^3$. Modeling a line of receptors 150 m long to represent the pedestrian walkway, as shown in Figure 7, results in a period average of 4.27 $\mu g/m^3$. Using either analysis, with a single receptor or multiple receptors, it can be concluded that modeled estimates indicate that a pedestrian may experience 75 percent of the impact of the BOTA emissions relative to the concentrations inside the BOTA. Furthermore, the entire pedestrian walkway runs alongside the BOTA within 10 m of the edge of the lanes. It is seen in the concentration exposure heat maps that pollutant concentrations within 10 m, along the side of the traffic lanes, remain at elevated levels at around 80 percent of those inside the traffic lanes. The concentration heat map, therefore, is a useful tool as guidance for placing pedestrian walkways or other points of exposure to individuals and workers. Other discrete receptors modeled include the office location, the WestPedestrian walkway, and the Southbound Toll Booth (SBToll). The SBtoll and WestPedestrian receptors were both located to the west of the main entrance to the U.S. lanes and at least 25 m away from the congested traffic lanes going northbound. The modeled period-average concentrations at both these receptors were around 75 percent less than the concentration estimates inside the BOTA. Concentration estimates at the main office receptor were also around 75 percent less than the concentration estimates inside the BOTA.

The air dispersion model results indicate that, overall, the emissions from the BOTA have a small impact on the community near the POE. The impact on the community in this case is measured by the estimates of pollutant concentrations at those receptors that represent the school sites on both sides of the border. When comparing modeled concentrations versus the observed monitored concentrations at the school sites using low-cost sensors, it is seen that the period-averaged modeled concentrations account for around 1–2 percent of monitored concentrations. The 1-hr max modeled concentrations of $PM_{2.5}$ are around 2 percent of monitored concentrations. However, for two schools nearest to the BOTA, modeled 1-hr max concentrations account for 11 percent of monitored concentrations. At these two school sites, Zavala and CJ5-H, modeled concentrations also account for 5 percent of monitored 24-hr max concentrations. This indicates that while the impact of the BOTA traffic-related emissions is low, it may be observed during 1-hr or 24-hr time periods when wind speeds are low. This may also be due to the sensitivity of the low-cost sensors, which require further study and calibration.

These modeled concentrations are highly influenced by the input parameters used in modeling. This study used winter emissions rates for vehicles traveling on urban-arterial roads at 2.5 mph. However, future models may consider using emissions rates for idling vehicles or vehicles traveling on different road types such as urban-arterial, rural-freeway, or rural-arterial. When applying the ERs for idling and 2.5-mph speeds on the same road type (urban-arterial) we observe that for the three pollutants, 2.5-mph ERs are greater than those for idling. NO_2 ERs at 2.5 mph are two times higher than at idling. Additionally, $PM_{2.5}$ ERs for vehicles traveling at 2.5 mph are five times higher than those for idling, and PM_{10} ERs at 2.5 mph are 30 times higher than at idling. Considering these factors, using an idling ER for PM_{10} would result in much lower concentration estimates. This study chose to model 2.5-mph ERs to represent the slow and constant flow of vehicles queuing at the BOTA in order to average the many scenarios of traffic flow occurring over the study period.

Summary and Future Research

We conducted a 1-month air monitoring campaign at the BOTA in El Paso, Texas, using three continuous FEM instruments for three criteria pollutants ($PM_{2.5}$, O_3, and NO_2) to assess the levels of exposure to the facility operators and users of the BOTA with in-traffic monitoring. Concurrent monitoring of PM ($PM_{2.5}$ and PM_{10}) in the nearby community was performed using a number of low-cost PM sensors to provide citizens with real-time PM pollution levels. These low-cost sensors were located at elementary schools on both sides of the U.S.-Mexico border. Assessment of the low-cost sensor data was conducted using multiple linear regression analysis and simple linear regression analysis calibrated against reference data. Air dispersion modeling was conducted using the state-of-the-art seasonal traffic-related emission rates estimated for the BOTA and real-time surface meteorological data obtained from a nearby weather station to predict the $PM_{2.5}$, PM_{10}, and NO_2 levels at the BOTA and the surrounding areas. Comparison of these modeled concentration estimates and the monitored concentrations provide insight into the contribution of BOTA traffic-related emissions to the ambient pollutant concentrations.

We quantified the exposure concentrations of $PM_{2.5}$, PM_{10}, O_3, and NO_2 for the BOTA workers, users, and pedestrians. Concurrent FRM hourly $PM_{2.5}$, O_3, and NO_2 data recorded at a state-operated continuous air monitoring station located within 0.4 km of the BOTA were reviewed and compared to the concentrations discovered in our study. The performance of all three FEM devices was determined to be in excellent agreement with that of the collocated FRM instruments. However, the performance and accuracy of the low-cost sensors appear to be less reliable during our study, although the devices were capable of detecting the trends and variability of pollutant concentrations in real time. These low-cost sensors also provided concentration estimates and trends to the general public with data available online throughout the duration of the study. Our results showed that in-traffic air pollutant concentrations at a busy international POE do not exceed their respective NAAQs. It is important to keep in mind that NAAQs are established for yearly or long-term evaluations and this study was conducted for around one month. Additionally, monitored all-period averaged concentrations at the BOTA of $PM_{2.5}$, O_3, and NO_2 were found to be 2 percent higher, 15 percent lower, and 20 percent higher, respectively, than the concentrations observed at a nearby reference station only 0.4 km away (CAMS 41). Higher levels of NO_2 inside the BOTA are expected due to the fact that NO_2 is primarily released in the air through the burning of fuels from vehicles and trucks. Occasional emission spikes due to sudden prolonged wait time, adverse meteorological conditions due to low wind conditions and temperature emissions, and dust events due to high wind conditions (for $PM_{2.5}$ and PM_{10} only) were likely to cause short-term (5-minutes) concentration spikes.

The air dispersion modeling of the POE wait time on pollution levels at the BOTA showed that modeled on-site air pollution stabilizes to a maximum at a queue length of approximately 270 m. The BOTA operators deployed at the POE are expected to be exposed to the maximum levels of pollution when the queue length exceeds 270 m from the toll booth locations. These maximum modeled pollution levels for $PM_{2.5}$, PM_{10}, NO_2, and O_3 are less than their respective NAAQs. In addition, modeled air pollution disperses rapidly as the lateral distance from the center of the BOTA increases. The modeled air pollutant concentrations decrease by approximately tenfold as the cross-BOTA distance increases to 200 m, indicating that pedestrians and near-road BOTA workers should maintain distances up to this level to experience less impact from the BOTA traffic-related emissions. Modeled estimates indicate that individuals traveling along the pedestrian walkway may experience 75 percent of the impact of the BOTA emissions relative to the concentrations inside the BOTA. The modeled BOTA emissions were found to contribute 51 percent, 147 percent, and 7 percent of the monitored all-period averaged $PM_{2.5}$, PM_{10}, and NO_2 concentrations, respectively, as shown in Table 13. Modeled concentration estimates also indicate that toll booth workers experience 66 percent of the pollutant concentrations estimated inside the traffic lanes of the BOTA. Modeled concentration estimates also provide a spatial heat map to assess the reach and direction of highest pollution exposure. Wind speeds coming from the southwest direction during this study period resulted in a higher impact of the emissions from the BOTA to those receptors downwind of the BOTA, north and east of the traffic lanes.

AERMOD, the atmospheric dispersion modeling system that is used to estimate the concentration of air pollutants emitted from pollution sources, was used to assess the impacts of the BOTA emissions on the community. Future research related to this study can expand on the modeling and dispersion parameters used in AERMOD. The dispersion model is greatly affected by the ERs used to estimate pollutant concentrations. This study used winter emissions rates for vehicles traveling on urban-arterial roads at 2.5 mph. However, future models may consider using emissions rates for idling vehicles or vehicles

traveling on different road types such as urban-arterial, rural-freeway, or rural-arterial. Future research may also focus on expanding community monitoring and establishing background concentrations for the area. This study found that concentrations monitored in traffic at the BOTA are very similar to those concentrations at TCEQ reference sites (particularly at CAMS 41, 37, 39), which indicate that the effect of the traffic at the BOTA resembles the pollutant concentrations observed over a larger geographic area affected by traffic emissions. In conclusion, this study provides border traffic exposures of the POE workers and users of three major air pollutants. Further research into this subject should reflect the factors described in this study, considering that cross-border air quality issues continue to pose a challenge in environmental justice for border crossers at POEs as well as neighboring populations on both sides of the border. Further studies at more POEs along the border will also help validate our findings.

References

2B Technologies, 2017a. NO2/NO/NOx Monitor Operation Manual.

2B Technologies, 2017b. Ozone Monitor Operation Manual.

Ardon-Dryer, K., Dryer, Y., Williams, J.N., Moghimi, N., 2020. Measurements of PM2.5 with PurpleAir under atmospheric conditions. Atmos. Meas. Tech. 13, 5441–5458. https://doi.org/10.5194/AMT-13-5441-2020

Baldauf, R., Thoma, E., Hays, M., Shores, R., Kinsey, J., Gullett, B., Kimbrough, S., Isakov, V., Long, T., Snow, R., Khlystov, A., Weinstein, J., Chen, F.L., Seila, R., Olson, D., Gilmour, I., Cho, S.H., Watkins, N., Rowley, P., Bang, J., 2008. Traffic and meteorological impacts on near-road air quality: Summary of methods and trends from the Raleigh near-road study. J. Air Waste Manag. Assoc. 58, 865–878. https://doi.org/10.3155/1047-3289.58.7.865

Barkjohn, K.K., Gantt, B., Clements, A.L., 2021. Development and application of a United States-wide correction for PM 2.5 data collected with the PurpleAir sensor. Atmos. Meas. Tech 14, 4617–4637. https://doi.org/10.5194/amt-14-4617-2021

Baxter, L.K., Barzyk, T.M., Vette, A.F., Croghan, C., Williams, R.W., 2008. Contributions of diesel truck emissions to indoor elemental carbon concentrations in homes in proximity to Ambassador Bridge. Atmos. Environ. 42, 9080–9086. https://doi.org/10.1016/j.atmosenv.2008.09.023

Branco, P.T.B.S., Alvim-Ferraz, M.C.M., Martins, F.G., Sousa, S.I. V, 2014. The microenvironmental modelling approach to assess children's exposure to air pollution - A review. Environ. Res. 135, 317–332. https://doi.org/10.1016/j.envres.2014.10.002

Chen, L.-W.A., Tropp, R.J., Li, W.-W., Zhu, D., Chow, J.C., Watson, J.G., Zielinska, B., 2012. Aerosol and Air Toxics Exposure in El Paso, Texas: A Pilot Study. Aerosol Air Qual. Res. 12, 169–179. https://doi.org/10.4209/aaqr.2011.10.0169

Cyrys, J., Heinrich, J., Hoek, G., Meliefste, K., Lewné, M., Gehring, U., Bellander, T., Fischer, P., Vliet, P. van, Brauer, M., Wichmann, H.-E., Brunekreef, B., 2003. Comparison between different traffic-related particle indicators: Elemental carbon (EC), PM2.5 mass, and absorbance. J. Expo. Sci. Environ. Epidemiol. 13, 134–143. https://doi.org/10.1038/sj.jea.7500262

Galaviz, V.E., Yost, M.G., Simpson, C.D., Camp, J.E., Paulsen, M.H., Elder, J.P., Hoffman, L., Flores, D., Quintana, P.J.E., 2014. Traffic pollutant exposures experienced by pedestrians waiting to enter the U.S. at a major U.S.–Mexico border crossing. Atmos. Environ. 88, 362–369. https://doi.org/10.1016/j.atmosenv.2013.12.042

GRIMM, 2010. Specification for portable laser aerosol spectrometer and dust monitor model 1.108/1.109. Users Man. 11.

HEI, 2010. Traffic-Related Air Pollution: A Critical Review of the Literature on Emissions, Exposure, and Health Effects A Special Report of the HEI Panel on the Health Effects of Traffic-Related Air Pollution - Executive Summary. Heal. Eff. Inst.

Janssen, N.A.H., Vliet, P.H.N. Van, Harssema, H., Brunekreef, B., 2001. Assessment of exposure to traffic related air pollution of children attending schools near motorways 35, 3875–3884.

Kelly, K.E., Whitaker, J., Petty, A., Widmer, C., Dybwad, A., Sleeth, D., Martin, R., Butterfield, A., 2017. Ambient and laboratory evaluation of a low-cost particulate matter sensor. Environ. Pollut. 221, 491–500. https://doi.org/10.1016/j.envpol.2016.12.039

Kelly, K.E., Xing, W.W., Sayahi, T., Mitchell, L., Becnel, T., Gaillardon, P.-E., Meyer, M., Whitaker, R.T., 2021. Community-Based Measurements Reveal Unseen Differences during Air Pollution Episodes. Environ. Sci. Technol. 55, 120–128.

https://doi.org/10.1021/acs.est.0c02341

Kim, H.H., Lee, C.S., Yu, S. Do, Lee, J.S., Chang, J.Y., Jeon, J.M., Son, H.R., Park, C.J., Shin, D.C., Lim, Y.W., 2016. Near-road exposure and impact of air pollution on allergic diseases in elementary school children: A cross-sectional study. Yonsei Med. J. 57, 698–713. https://doi.org/10.3349/ymj.2016.57.3.698

Li, W.W., Orquiz, R., Garcia, J.H., Espino, T.T., Pingitore, N.E., Gardea-Torresdey, J., Chow, J., Watson, J.G., 2001. Analysis of temporal and spatial dichotomous PM air samples in the El Paso-Cd. Juarez air quality basin. J. Air Waste Manag. Assoc. 51, 1551–1560. https://doi.org/10.1080/10473289.2001.10464377

Magi, B.I., Cupini, C., Francis, J., Green, M., Hauser, C., 2020. Evaluation of PM2.5 measured in an urban setting using a low-cost optical particle counter and a Federal Equivalent Method Beta Attenuation Monitor. Aerosol Sci. Technol. 54, 147–159. https://doi.org/10.1080/02786826.2019.1619915

Miller, L., Lemke, L.D., Xu, X., Molaroni, S.M., You, H., Wheeler, A.J., Booza, J., Grgicak-Mannion, A., Krajenta, R., Graniero, P., Krouse, H., Lamerato, L., Raymond, D., Reiners, J., Weglicki, L., 2010. Intra-urban correlation and spatial variability of air toxics across an international airshed in Detroit, Michigan (USA) and Windsor, Ontario (Canada). Atmos. Environ. 44, 1162–1174. https://doi.org/10.1016/j.atmosenv.2009.12.030

Olvera, H.A., Li, W.-W., Garcia, H., 2011. Air quality characterization at the Mexican customs inspection area at the international bridge of the Americas. San Diego, CA.

Olvera, H.A., Lopez, M., Guerrero, V., Garcia, H., Li, W.-W., 2013. Ultrafine particle levels at an international port of entry between the US and Mexico: Exposure implications for users, workers, and neighbors. J. Expo. Sci. Environ. Epidemiol. 23, 289–298. https://doi.org/10.1038/jes.2012.119

Quintana, P.J.E., Dumbauld, J.J., Garnica, L., Chowdhury, M.Z., Velascosoltero, J., Mota-Raigoza, A., Flores, D., Rodríguez, E., Panagon, N., Gamble, J., Irby, T., Tran, C., Elder, J., Galaviz, V.E., Hoffman, L., Zavala, M., Molina, L.T., 2014. Traffic-related air pollution in the community of San Ysidro, CA, in relation to northbound vehicle wait times at the US–Mexico border Port of Entry. Atmos. Environ. 88, 353–361. https://doi.org/10.1016/j.atmosenv.2014.01.009

Quintana, P.J.E., Ganster, P., Stigler Granados, P.E., Muñoz-Meléndez, G., Quintero-Núñez, M., Rodríguez-Ventura, J.G., 2015. Risky Borders: Traffic Pollution and Health Effects at US–Mexican Ports of Entry. J. Borderl. Stud. 30, 287–307. https://doi.org/10.1080/08865655.2015.1066697

Quintana, P.J.E., Khalighi, M., Castillo Quiñones, J.E., Patel, Z., Guerrero Garcia, J., Martinez Vergara, P., Bryden, M., Mantz, A., 2018. Traffic pollutants measured inside vehicles waiting in line at a major US-Mexico Port of Entry. Sci. Total Environ. 622–623, 236–243. https://doi.org/10.1016/j.scitotenv.2017.11.319

Raysoni, A.U., Sarnat, J.A., Sarnat, S.E., Garcia, J.H., Holguin, F., Luèvano, S.F., Li, W.-W., 2011. Binational school-based monitoring of traffic-related air pollutants in El Paso, Texas (USA) and Ciudad Juárez, Chihuahua (México). Environ. Pollut. 159, 2476–2486. https://doi.org/10.1016/j.envpol.2011.06.024

Raysoni, A.U., Stock, T.H., Sarnat, J.A., Chavez, M.C., Sarnat, S.E., Montoya, T., Holguin, F., Li, W.W., 2017. Evaluation of VOC concentrations in indoor and outdoor microenvironments at near-road schools. Environ. Pollut. 231, 681–693. https://doi.org/10.1016/j.envpol.2017.08.065

Sharma, A., Massey, D.D., Taneja, A., 2009. Horizontal gradients of traffic related air pollutants near a major highway in Agra, India. IJRSP Vol.38(6) [December 2009] 38, 338–346.

Smit, R., Kingston, P., Neale, D.W., Brown, M.K., Verran, B., Nolan, T., 2019. Monitoring on-road air quality and measuring vehicle emissions with remote sensing in an urban area. Atmos. Environ. 218, 116978.

https://doi.org/10.1016/j.atmosenv.2019.116978

Texas A&M Transportation Institute, 2022. Development of Emission Rate Lookup Tables (ERLTs). Austin, Texas.

Tong, H.Y., Hung, W.T., Cheung, C.S., 2000. On-road motor vehicle emissions and fuel consumption in urban driving conditions. J. Air Waste Manag. Assoc. 50, 543–554. https://doi.org/10.1080/10473289.2000.10464041

Tryner, J., L'Orange, C., Mehaffy, J., Miller-Lionberg, D., Hofstetter, J.C., Wilson, A., Volckens, J., 2020. Laboratory evaluation of low-cost PurpleAir PM monitors and in-field correction using co-located portable filter samplers. Atmos. Environ. 220, 117067. https://doi.org/10.1016/j.atmosenv.2019.117067

U.S. Customs and Border Protection, 2022. Border Wait Times [WWW Document]. URL https://bwt.cbp.gov/historical (accessed 3.24.23).

U.S. EPA, 2015. Transportation Conformity Guidance for Quantitative Hot-spot Analyses in PM2.5 and PM10 Nonattainment and Maintenance Areas. Office of Transportation and Air Quality.

Zora, J.E., Sarnat, S.E., Raysoni, A.U., Johnson, B.A., Li, W.W., Greenwald, R., Holguin, F., Stock, T.H., Sarnat, J.A., 2013. Associations between urban air pollution and pediatric asthma control in El Paso, Texas. Sci. Total Environ. 448, 56–65. https://doi.org/10.1016/j.scitotenv.2012.11.067